Molecular Pharmacology Fast Forward. Published on July 7, 2014 as doi:10.1124/mol.114.093377

The novel α7β2-nicotinic acetylcholine receptor subtype is expressed in mouse and human basal forebrain: Biochemical and pharmacological characterisation

Milena Moretti, Michele Zoli, Andrew A George, Ronald J Lukas, Francesco Pistillo, Uve Maskos, Paul Whiteaker, and Cecilia Gotti

CNR, Neuroscience Institute-Milano, Biometra University of Milan, Milan, Italy (MM ,FP, CG; Primary Laboratory of Origin).

Department of Biomedical, Metabolic and Neural Sciences, section of Physiology and Neurosciences, University of Modena and Reggio Emilia, Modena, Italy (MZ).

Division of Neurobiology, Barrow Neurological Institute, Phoenix AZ 85013, USA (AAG, RJL, PW).

Centre National de la Recherche Scientifique, Unité Neurobiologie Intégrative des Systèmes Cholinergiques, Institut Pasteur, 75724 Paris Cedex 15, France (UM).

Molecular Pharmacology Fast Forward. Published on July 7, 2014 as DOI: 10.1124/mol.114.093377
This article has not been copyedited and formatted. The final version may differ from this version.

RUNNING TITLE: Human α7β2-nAChR human expression & functional pharmacology.

Corresponding authors: Cecilia Gotti, Ph.D.

CNR, Neuroscience Institute

Via Vanvitelli 32, 20129 Milan, Italy

Tel +39 02 50316974, Fax +39 02 50317132

Email: c.gotti@in.cnr.

Paul Whiteaker, Ph.D.

Division of Neurobiology, Barrow Neurological Institute

St. Joseph's Hospital and Medical Center

350 W. Thomas Rd.

Phoenix, AZ 85013, USA

Tel +1 602 406 6534, Fax +1 602 406 4172

Email: paul.whiteaker@dignityhealth.org.

Text pages: 45 (not including supplementary data)

Tables: 5

Figures: 5

References: 59

Abstract: 224

Introduction: 711

Discussion: 1696

Non-standard abbreviations: α-Bgtx, α-bungarotoxin; α-Cbtx, α-cobratoxin; AD, Alzheimer's disease; C C4, 1,2-bis-N -cystinylethane; DHβE, dih ydro-β-erythroidine; E pi, epibatidine; MECA, mecamylamine; MLA, methyllycaconitine; nAChR, nicotinic acetylcholine receptor(s); PMSF, phenylmethylsuphonylfluoride; SDS-PAGE, sodium dodecyl sulphate-polyacrylamide gel electroph oresis; SN/VTA, substantia nigra / ventral tegmental area; TBS, Tris-buffered saline;

TEVC, two-electrode voltage-clamp.

Molecular Pharmacology Fast Forward. Published on July 7, 2014 as DOI: 10.1124/mol.114.093377
This article has not been copyedited and formatted. The final version may differ from this version.

ABSTRACT:

We examined α7β2-nicotinic acetylcholine receptor (α7β2-nAChR) expression in mammalian brain and compared pharmacological profiles of homomeric α7-nAChR and of α7β2-nAChR. α-bugarotoxin affinity purification or immunoprecipitation with anti-α7 subunit antibodies (Abs) were used to isolate nAChR containing α7 subunits from mouse or human brain samples. α7β2-nAChR were detected in forebrain, but not other tested regions, from both species, based on western blot analysis of isolates using β2 subunit- specific Abs. Ab specificity was confirmed in control studies using subunit-null mutant mice or cell lines heterologously expressing specific, human nAChR subtypes and subunits. Functional expression in Xenopus oocytes of concatenated pentameric $(\alpha7)_5$-, $(\alpha7)_4(\beta2)_1$-, and $(\alpha7)_3(\beta2)_2$-nAChR was confirmed using two-electrode voltage-clamp recording of responses to nicotinic ligands. Importantly pharmacological profiles were indistinguishable for concatenated $(\alpha7)_5$-nAChR or for homomeric α7-nAChR constituted from unlinked α7 subunits. Pharmacological profiles were similar for $(\alpha7)_5$-, $(\alpha7)_4(\beta2)_1$-, and $(\alpha7)_3(\beta2)_2$-nAChR except for diminished efficacy of nicotine (normalized to acetylcholine efficacy) at α7β2- *vs.* α7-nAChR. This study represents the first direct confirmation of α7β2-nAChR expression in human and mouse forebrain, supporting previous mouse studies that suggested relevance of α7β2-nAChR in Alzheimer's disease etiopathogenesis. These data also indicate that α7β2-nAChR subunit isoforms with different α7:β2 subunit ratios have similar pharmacological profiles to each other, and to α7 homopentameric nAChR. This supports the hypothesis that α7β2-nAChR agonist activation predominantly or entirely reflects binding to α7/α7 subunit interface sites.

Molecular Pharmacology Fast Forward. Published on July 7, 2014 as DOI: 10.1124/mol.114.093377
This article has not been copyedited and formatted. The final version may differ from this version.

INTRODUCTION

Several nicotinic acetylcholine receptor (nAChR) subtypes are expressed widely along the entire neuraxis, and are involved in many of the physiological functions of the central and peripheral nervous systems (Albuquerque et al., 2009; Hurst et al., 2013). nAChR activity controls important aspects of synaptic function and brain development, including the proliferation and differentiation of neural progenitors, neuronal migration, and neuronal maturation (Griguoli and Cherubini, 2012; Picciotto et al., 2012; Yakel, 2013). Furthermore, nAChR dysfunction may play an important role in a variety of neurological diseases including neurodegenerative and psychiatric diseases (Gotti and Clementi, 2004; Lewis and Picciotto, 2013).

α4β2- and homomeric α7-nAChR are the most widely-expressed subtypes in mammalian brain. The latter are thought to contain five identical agonist binding sites located at subunit interfaces in extracellular domains (Gotti and Clementi, 2004; Whiteaker et al., 2007). Pharmacological hallmarks of α7-nAChR are their high sensitivity to antagonism by snake venom-derived polypeptide toxins such as α-bungarotoxin (α-Bgtx) and α-cobratoxin (α-Cbtx), and their sensitivity to choline (a product of ACh hydrolysis) as an agonist (Albuquerque et al., 1997; Albuquerque et al., 2009). α7-nAChR are highly expressed in the cortex, hippocampus and subcortical limbic regions, and (at lower levels) in the thalamus and basal ganglia. α7-nAChR that are located on or near nerve terminals are involved in control of neurotransmitter release, whereas α7-nAChR on dendrites or soma apposed to cholinergic synaptic endings play roles in classic neurotransmission. In both cases, α7-nAChR's high calcium permeability may also result in altered intracellular signalling and gene transcription (Albuquerque et al., 2009; Dajas-Bailador and Wonnacott, 2004). α7-nAChR also may be associated with extrasynaptic volume transmission (Lendvai and Vizi, 2008).

Affinity purification of nAChR using snake-venom α-toxins has been performed from brain tissue of various species. Extracts from whole rat brain appear to be predominantly

Molecular Pharmacology Fast Forward. Published on July 7, 2014 as DOI: 10.1124/mol.114.093377
This article has not been copyedited and formatted. The final version may differ from this version.

composed of homomeric α7-nAChR (Drisdel and Green, 2000). However homomeric α7- and α8-nAChR (and heteromeric α7α8-nAChR) have been identified in chick CNS extracts (Gotti et al., 1994; Keyser et al., 1993). Further, studies using heterologous systems have shown that α7 subunits can form functional channels when combined with α5 (Girod et al., 1999), β2 (Khiroug et al., 2002), β3 (Palma et al., 1999) or β4 subunits (Criado et al., 2012). Fluorescently tagged nAChR α7 and β2 subunits have recently been used to characterize the formation of α7β2-nAChR, and functional differences between α7- and α7β2-nAChR have been suggested (Murray et al., 2012). Co-expression of β2 and α7 subunits caused a significant decrease in agonist-evoked whole cell current amplitudes, but this decrease occurs without affecting the concentration-response characteristics of a range of common agonists and antagonists (Murray et al., 2012). Other studies have shown that α7 and β2 subunits are co-expressed in rat basal forebrain cholinergic neurons and appear to form heteromeric α7β2-nAChR with subtly different biophysical and pharmacological properties from those of homomeric α7-nAChR (Liu et al., 2009). In addition, interaction of these putative α7β2-nAChR with oligomeric forms of amyloid-β (Aβ1-42) may be relevant in the etiology of Alzheimer's disease (Liu et al., 2013).

These previous studies suggest that the function and pharmacology of α7*-nAChR (where * denotes the known or possible presence of other nAChR subunits than α7 (Lukas et al., 1999)) may be more complex than previously thought, and that α7β2-nAChR expression may be restricted to forebrain areas. However, heteromeric α7*-nAChR have not yet been directly detected biochemically, nor have they been definitively identified in human brain. We used the α7-nAChR-selective ligand, α-Bgtx, to affinity purify α7*-nAChR from selected brain areas of humans or of wildtype (WT) or β2 subunit-null mutant (KO) mice. The subunit compositions of these isolated α7*-nAChR were analyzed by western blot analysis using subunit-specific anti- α7 or β2 antibodies. The results show expression of α7β2-nAChR in both WT mouse and human forebrain samples, but not in brains from β2 KO mice. Moreover, concatemeric (linked subunit) constructs, the Xenopus oocyte system, and two-

Molecular Pharmacology Fast Forward. Published on July 7, 2014 as DOI: 10.1124/mol.114.093377
This article has not been copyedited and formatted. The final version may differ from this version.

electrode voltage-clamp recordings were used to confirm functional expression of α7β2-nAChR. This work defined α7 and β2 subunit stoichiometries that enable α7β2-nAChR function, and showed similar pharmacological characteristics across α7- and α7β2 nAChR subtypes. The results confirm commonalities in expression of α7β2-nAChR in man and mouse, and support hypotheses linking α7β2-nAChR, cholinergic signaling loss, and roles for Aβ1-42 in etiopathogenesis of at least a subset of human dementias.

Molecular Pharmacology Fast Forward. Published on July 7, 2014 as DOI: 10.1124/mol.114.093377
This article has not been copyedited and formatted. The final version may differ from this version.

MATERIALS and METHODS

Animals and Materials

The study involved the use of 4-6 month old male, pathogen-free, C57BL/6 wildtype (WT), α7 KO or β2 KO (Orr-Urtreger et al., 1997; Picciotto et al., 1995) mice obtained from Dr. U. Maskos (Pasteur Institute, Paris). All animal experiments were conducted in accordance with the European Community Council Directive (86/609/EEC) of 24 November 1986.

(±)-[^{3}H]-epibatidine (Epi, specific activity, 66Ci/mmol) and [^{125}I]-α-Bgtx (specific activity of 200-216 Ci/mmol) were purchased from Perkin Elmer (Waltham, MA, USA). Non-radioactive α-Bgtx, Epi, and nicotine were purchased from Tocris Bioscience (Bristol, UK or Minneapolis, MN, USA), as were dihydro-β-erythroidine (DHβE), and methyllycaconitine (MLA). Sazetidine-A (also known as AMOP-H-OH) was kindly supplied by Dr. Alan Kozikowski (University of Illinois at Chicago, Chicago, IL, USA). 1,2-bis Ncytisinylethane (CC4) also was used (Riganti et al., 2005). α-Cobratoxin (α-Cbtx) and all other reagents were sourced from Sigma-Aldrich unless otherwise specified (St. Louis, MO, USA).

Human tissues

Human cerebellum was provided by the Newcastle Brain Tissue Resource on the basis of a collaboration with Dr Jennifer Court (Newcastle upon Tyne, General Hospital, UK). Samples were all collected by the Brain Tissue Resource with informed consent and appropriate ethical approval. Case details are shown in Table 1; the approvals and method for categorizing the subjects' smoking status are outlined in the methods section of Court et al., 2005. Human basal forebrain tissue was provided by Dr. Emanuele Sher (Lilly Research Center, Windlesham, Surrey, UK), and was also collected with appropriate informed consent in accordance with all applicable laws and regulations.

Transfected cells

Human α2, α3, β2, and β4 nAChR subunit clones in the mammalian expression vector pcDNA3 were kind gifts of Dr. Sergio Fucile (University of Rome, Rome, Italy). The

Molecular Pharmacology Fast Forward. Published on July 7, 2014 as DOI: 10.1124/mol.114.093377
This article has not been copyedited and formatted. The final version may differ from this version.

human α7 nAChR subunit clone in pcDNA3 was a generous gift of Dr. Roberta Benfante (CNR Institute of Neuroscience, Milan, Italy). HEK293 and SH-SY5Y cells were transiently transfected using the $Ca_3(PO4)_2$ method or the Jet-PEI reagent (Polyplus, Euroclone, Italy) transfection. For the α7 plasmid, $1.5x10^6$ cells were transfected with 6 μg of plasmid using the Jet-PEI. For each of the α2, α3, α4 and β2 or β4 subunit 20 μg of plasmids for $1.5x10^6$ cells was used, with the $Ca_3(PO4)_2$ method. nAChR expression by cells was analyzed 24 h after transfection.

Antibody Production and Characterization

We used affinity-purified, subunit-specific, polyclonal antibodies (Abs), produced in rabbit against peptides derived from the C-terminal (COOH) or intracytoplasmic loop (CYT) of human or mouse nAChR subunit sequences, as previously described (Gotti et al., 2006; Grady et al., 2009). The Ab against the COOH peptide (SAPNFVEAVSKDFA) was used for α7 subunits in mouse and human tissues. Abs directed against the α7 mouse CYT peptide (PSGDPDLAKILEEVRYIANRFRC) or the human CYT peptide (QMQEADISGYIPNGQMQEADISGYIPNG) were used for mouse and human tissues, respectively. For the β2 subunit, we used antibodies directed against two different cytoplasmic human β2 peptides: RQREREGAGALFFREAPGADSCTY (β2(1)) and cgIADHMRSEDDDQSVREDWKYV (β2(2)).

The specificity of the affinity-purified Abs was tested by immunoprecipitation studies using α7 WT or α7 KO hippocampus and β2 WT or β2 KO mouse cortex (the results are shown in Supplementary Figure 1). The same Abs also were tested by means of western blotting (Supplementary Figure 1). In order to exclude any cross-reactivity between nAChR subunits, anti-β2 (1)- or anti- α7 human subunit Abs were also tested by means of immunoprecipitation studies and western blotting in HEK293 cells transfected to express human α2β4-, α4β2-, α4β4, or α3β4-nAChR subtypes or in SH-SY5Y cells transfected to express human α7-nAChR (see above) (the results are shown in Supplementary Figure 2).

Purification of α-bungarotoxin-binding nAChR

Molecular Pharmacology Fast Forward. Published on July 7, 2014 as DOI: 10.1124/mol.114.093377
This article has not been copyedited and formatted. The final version may differ from this version.

For studies using mice, ≈100 mg of basal forebrain or hippocampus tissue micro-dissected from either WT or subunit-null mice were pooled in every experiment. The tissue was homogenised in 10 ml of 50 mM Na phosphate, pH 7.4, 1 M NaCl, 2 mM EDTA, 2 mM EGTA and 2 mM phenylmethylsufonylfluoride (PMSF; to covalently inactivate serine protease activity), and the homogenates were diluted and centrifuged for 1.5 h at 60,000g. The entire membrane homogenisation, dilution and centrifugation procedure was then repeated, and the resulting pellets were collected, rapidly rinsed with 50 mM Tris HCl, pH 7, 120 mM NaCl, 5 mM KCl, 1 mM $MgCl_2$, 2.5 mM $CaCl_2$ and 2 mM PMSF. The washed pellets were then resuspended in 2 ml of the same buffer, further supplemented with 20 µg/ml of each of the following protease inhibitors: leupeptin, bestatin, pepstatin A and aprotinin. Triton X-100 at a final concentration of 2% was added to the washed membranes, which were extracted for 2 h at 4° C. The extracts were centrifuged for 1.5 h at 60,000g, recovered, and an aliquot of the supernatants was collected for protein measurement using the BCA protein assay (Pierce Biotechnology, Inc., Rockford, IL, USA), with bovine serum albumin as the standard. Extracts (2 ml) were incubated with 200 µl of Sepharose-α-Bgtx (concentration of coupled toxin 1 mg/ml of gel) and shaken overnight at 4 °C. The following day, the beads were centrifuged, the supernatant was recovered, and the resins were washed 4-6 times by resuspension followed by centrifugation. After washing, the Sepharose-α-Bgtx beads with bound nAChR (purified α-Bgtx-binding receptors) were incubated with one-two volumes of Laemmli sample buffer (125 mM Tris phosphate, 4% SDS, 20% glycerol, 0,02 % bromophenol blue and 10% 2-mercaptoethanol pH 6.8) and boiled for 2 min. The supernatant was then recovered by centrifugation.

In the case of human tissue, α-Bgtx-binding sites were purified using the same procedure as that used for mouse tissue, starting from 600 mg of tissue (See Table 1 for subject details).

Binding studies

[^{125}I]-α-Bungarotoxin

Molecular Pharmacology Fast Forward. Published on July 7, 2014 as DOI: 10.1124/mol.114.093377
This article has not been copyedited and formatted. The final version may differ from this version.

The binding of [^{125}I]-α-Bgtx to 2% Triton X-100 extracts of mouse tissues was determined by collection onto DEAE-Sepharose™ Fast Flow (GE Healthcare, Uppsala, Sweden). Triton extracts (250 µl) from each experimental group were incubated overnight with a saturating concentration (5 nM) of [^{125}I]-α-Bgtx at 20°C in the presence of 2 mg/ml bovine serum albumin. Specific radioligand binding was defined as total binding minus the non-specific binding determined in the presence of 1 µM unlabeled α-Bgtx. Non-specific binding averaged 30-40% of total binding. Binding to α7*-nAChR could also be measured in an immunoprecipitation assay format. Receptor extracts were labeled with [^{125}I]-α-Bgtx (5 nM in the presence or absence of 1 µM unlabeled α-Bgtx to define total and non-specific binding). The labelled extract could then be bound to protein A beads via anti-α7 subunit Abs (described later in Methods). Similar amounts of specific binding were recorded in either assay format, and non-specific binding was between 10-15% of total binding.

[^{3}H]-Epibatidine.

Binding of [^{3}H]-epibatidine to nAChR in 2% Triton X-100 brain tissue extracts obtained was also assessed. [^{3}H]-Epibatidine binds to multiple heteromeric nAChR subtypes with pM affinity and to α7-nAChR with nM affinity. In order to ensure that the α7 nAChR did not contribute to [^{3}H]-Epibatidine binding, in solubilized extracts, binding was performed in the presence of 1 µM α–Bgtx, which specifically binds to α7 nAChR (and thus prevents [^{3}H]-Epibatidine binding to these sites).

As for [^{125}I]-α-Bgtx binding assays, binding sites were captured using DEAE-Sepharose™ Fast flow, following overnight incubation of 250 µl aliquots of the extracts with 1 nM [^{3}H]-Epi at 4°C). Non-specific binding (averaging 5-10% of total binding) was determined in parallel samples containing 100 nM unlabelled Epi.

Immunoprecipitation

For immunoprecipiation studies of heteromeric receptors present in human tissues, we used Abs specific for α2, α3, α4, α5, β2 or β4 subunits directed against human subunit peptides as previously described (Gotti et al., 2006). For α6 and β3 subunits, we used Abs

Molecular Pharmacology Fast Forward. Published on July 7, 2014 as DOI: 10.1124/mol.114.093377
This article has not been copyedited and formatted. The final version may differ from this version.

directed against peptides of mouse subunit sequences, also as previously characterized and described (Grady et al., 2009). The immunoprecipitation capacities of the anti-human subunit Abs ranged from 90% to 100 % of the [^{3}H]-Epi labelled receptors (mean of three independent experiments). For immunoprecipitation experiments, affinity purified Abs were covalently immobilized on agarose-Protein A beads at a concentration of 4 mg/ml of wet resin. Immunoprecipitation was then performed by adding 20 µl of agarose-Protein A beads with bound, affinity-purified Abs to 200 µl of 1 nM [^{3}H]-Epi-labeled extracts. After overnight incubation, immunoprecipitates were recovered by centrifugation and washed three times with phosphate-buffered saline containing 0.1% Triton X-100.

Immunoblotting and densitometric quantification of western blot bands

nAChR subunit contents of tissue extracts or of α-Bgtx-binding complexes were analysed by western blotting. For the extracts loaded before and after the purification 10 µg of proteins were loaded whereas for the α-Bgtx- purified receptors a constant volume (40 µl), that depending on the tissue, may represent 1/10 or 1/20 of the total recovered Laemmli sample buffer-eluted receptors was loaded onto a 9% acrylamide (Biorad, Hercules, CA, USA) gel and subjected to sodium dodecyl sulphate-polyacrylamide gel electrophoresis (SDS-PAGE). After SDS-PAGE, proteins were electrophoretically transferred to nitrocellulose membranes with 0.45 mm diameter pores (Schleicher and Schuell, Dassel, Germany). The blots were blocked overnight in 5% non-fat milk in Tris-buffered saline (TBS), washed in a buffer containing 5% non fat-milk and 0.3% Tween 20 in TBS, incubated for two hours with the primary antibody (1–2.5 mg/ml), and then incubated with the appropriate peroxidase conjugated secondary Abs (Sigma-Aldrich. St Louis, MO, USA). After 10 washes, peroxidase was detected using a chemiluminescent substrate (Pierce, Rockford, IL, USA). The signal intensity of the Western blot bands was measured using an Epson 4500 gel scanner. The developed films were scanned as a Tiff image in eight-bit gray scale format at a resolution setting of 300 dpi. All of the films obtained from the separate experiments were acquired in the same way and scanned in parallel with a calibrated optical density step tablet

Molecular Pharmacology Fast Forward. Published on July 7, 2014 as DOI: 10.1124/mol.114.093377
This article has not been copyedited and formatted. The final version may differ from this version.

from Stouffer (Stouffer Graphics Arts, Mishawaka, IN, USA).

The images were analyzed using National Institutes of Health ImageJ software (Schneider et al., 2012). The pixel values of the images were transformed to optical density values by the program using the calibration curve obtained by acquiring the calibrated tablet with the same parameters as those used for the images. The immunoreactive bands were quantified in four separate experiments for the mouse hippocampus and basal forebrain as previously described (Grady et al., 2009)

Concatameric α7*-nAChR constructs

Fully-pentameric nAChR concatemers were constructed from human nAChR subunit sequences. cDNAs encoding concatamers were created using the same subunit layout we have previously employed to encode high- and low-agonist-sensitivity α4β2*-nAChR isoforms and α3β4(α5[D/N])-nAChR (Eaton et al., 2014; George et al., 2012). Subunits were arranged in the order α7-α7-α7-α7-α7 (α7 homopentamer), α7-α7-β2-α7-α7 or α7-β2-α7-β2-α7. Kozac and signal peptide sequences were removed from all subunit sequences with the exception of subunits expressed in the first position of the concatamer. Subunits were linked by alanine-glycine-serine (AGS) repeats designed to provide a complete linker length (including the C-terminal tail of the preceding subunit) of 40 ± 2 amino acids. At the nucleotide level, linker sequences were designed to contain unique restriction sites that allow easy removal and replacement of individual α7 and β2 subunits. The protein sequences for the human nAChR subunits were encoded by synthetic nucleotide sequences optimized for expression systems (GeneArt, Life Technologies, Grand Island, NY, USA). Optimization included minimization of high GC content sequence segments, improved codon usage, reduction of predicted RNA secondary structure formation, and removal of sequence repeats and possible alternative start and splice sites. Sequences of all subunits, together with their associated partial linkers, were confirmed by DNA sequencing (GeneArt). Each concatamer was subcloned into the pSGEM oocyte high-expression vector (a kind gift of Dr. Michael Hollmann; Ruhr-Universitaet, Bochum, Germany). For comparison, homomeric α7-nAChR also were expressed from unlinked individual subunits (cDNA clone also synthesized

Molecular Pharmacology Fast Forward. Published on July 7, 2014 as DOI: 10.1124/mol.114.093377
This article has not been copyedited and formatted. The final version may differ from this version.

and optimized by GeneArt). The unlinked human α7 subunit cDNA also was subcloned into the pSGEM vector.

RNA synthesis

Plasmids containing concatameric α7-homopentameric or α7β2 nAChR constructs, or individual α7 nAChR subunits, were linearized with NheI (2 hrs at 37 °C), and the reaction mix was treated with proteinase K (30 minutes at 50 °C). cRNAs were transcribed using mMessage mMachine T7 kit (Applied Biosystems/Ambion, Austin, TX, USA). Reactions were treated with TURBO DNase (1U for 15 minutes at 37 °C) and cRNAs were purified using the Qiagen RNeasy Clean-up kit (Valencia, CA, USA). cRNA purity was confirmed on a 1% agarose gel and preparations were stored at -80 °C.

***Xenopus* oocytes and RNA injection**

Xenopus oocytes were purchased from Ecocyte Bioscience US (Austin, TX) and incubated upon arrival at 13° C. The tips of pulled glass micropipettes were broken to achieve an outer diameter of ~40 µm (resistance of 2-6 MΩ), and pipettes were used to inject 20-60 nl containing 10 ng of cRNA/oocyte. To improve functional expression of α7*-nAChR, Ric-3 mRNA was also co-injected (Halevi et al., 2002). A ratio of 1:50 Ric-3:α7 subunit mRNA by mass was determined to be optimally effective in pilot experiments (data not shown).

Two-electrode voltage-clamp recording of α7- and α7β2-nAChR function

Two-electrode voltage-clamp recordings were made at room temperature (20 °C) in oocyte saline (OR2) solution (containing 82.5 mM NaCl, 2.5 mM KCl, 5 mM HEPES, 1.8 mM CaCl2·2H2O, and 1 mM MgCl2·6H2O, pH 7.4). Seven to fourteen days after injection, *Xenopus* oocytes expressing concatenated α7*-nAChR were voltage clamped at −70 mV with an Axoclamp 900A amplifier (Molecular Devices, Sunnyvale, CA, USA). Recordings were sampled at 10 kHz (low-pass Bessel filter: 40Hz; high-pass filter: DC), and the resulting traces were saved to disk (Molecular Devices Clampex v10.2). Data from oocytes with leak currents (I_{leak}) > 50 nA were excluded from recordings.

Molecular Pharmacology Fast Forward. Published on July 7, 2014 as DOI: 10.1124/mol.114.093377
This article has not been copyedited and formatted. The final version may differ from this version.

Nicotinic receptor pharmacology

Fresh stock drug solutions (agonists: ACh, choline, nicotine, sazetidine and 1,2-bis N cytisinylethane (CC4); antagonists dihydro-β-erythroidine (DHβE), methyllycaconitine (MLA), mecamylamine (MECA) and α-Cbtx) were made daily and diluted as required. Agonists and antagonists were applied using a sixteen channel, gravity-fed, perfusion system with automated valve control (AutoMate Scientific, Inc.; Berkeley, CA, USA). All solutions were supplemented with atropine sulfate (1.5 μM) to ensure that muscarinic ACh receptor responses were blocked and thus not recorded. Oocytes expressing loose subunits and/or concatemeric α7- or α7β2-nAChR were perfused with nAChR agonists for 5 seconds with 60 second washout times between each subsequent application. Oocytes were preincubated with nAChR antagonists for 2 minutes prior to activation with ACh (10 mM; 5 seconds). For experiments using α-Cbtx, bath and drug solutions were supplemented with 0.1% BSA to reduce loss of this peptide ligand by adsorption to the TEVC apparatus.

Data analysis

The expression of [^{3}H]-Epi and [^{125}I]-α-Bgtx receptors and the subunit contents of the [^{3}H]-Epi receptors expressed in the mouse and human samples were statistically compared using unpaired t tests. In human cerebellum samples from smokers and non-smokers, results were compared using an unpaired t test. Statistical analyses were performed using GraphPad Prism 5.0 software (GraphPad Software, Inc., La Jolla, CA, USA).

For TEVC data, EC_{50} and IC_{50} values were determined from nAChR-mediated peak currents through non-linear least-squares curve fitting (GraphPad Prism 5.0) using unconstrained, monophasic logistic equations to fit all parameters, including Hill slopes. Desensitization / inactivation of α7*-nAChR currents in the presence of 10 mM (maximally-stimulating) ACh was also analyzed by non-linear least-squares curve fitting in Graph Pad Prism 5.0. These data were best fit by a two-phase exponential decay equation. One-way ANOVA was used to compare parameters between multiple groups in each case. Tukey's

Molecular Pharmacology Fast Forward. Published on July 7, 2014 as DOI: 10.1124/mol.114.093377
This article has not been copyedited and formatted. The final version may differ from this version.

multiple comparison test was used for *post-hoc* analysis in order to compare the means of three or more groups (GraphPad Prism 5.0).

Molecular Pharmacology Fast Forward. Published on July 7, 2014 as DOI: 10.1124/mol.114.093377
This article has not been copyedited and formatted. The final version may differ from this version.

RESULTS

α-Bgtx-binding sites in WT or β2 KO mice

In preliminary experiments, we analysed nAChR expression in 2% Triton X-100 extracts obtained from the hippocampus or basal forebrain of WT or β2 KO mice (Table 2). By two different approaches (immunoprecipitating [^{125}I]-α-Bgtx-labelled receptors using anti-α7 subunit Abs and by [^{125}I]-α-Bgtx binding to Triton extracts) we determined that the density of α7*–nAChR in mouse hippocampus is more than two times higher than that in murine basal forebrain. During α-Bgtx binding site purification, we determined that 85-95% of those sites in Triton X-100 extracts were bound by α-Bgtx-Sepharose 4B affinity resins, whereas more than 95% of high affinity [^{3}H]-Epi binding was recovered in the flow-through.

The densities of [^{3}H]-epibatidine-binding nAChR were similar between the two regions (Table 2). Elimination of β2 subunit expression dramatically reduced expression of [^{3}H]-epibatidine-binding nAChR in both regions, indicating that this binding is almost entirely due to β2*-nAChR. In contrast, [^{125}I]-α-Bgtx (α7*-nAChR) expression was not significantly different between WT and β2 KO mice in either hippocampus or basal forebrain.

Additionally, western blot analysis was performed on α-Bgtx binding sites affinity purified from the hippocampus of WT or β2 KO mice and probed with anti-α7 (top) or anti-β2 (bottom) subunit Abs (Fig. 1A). Confirming results from the binding studies, western blots also showed no significant differences in presumed α7*-nAChR levels (i.e., polypetide labeled with anti-α7 subunit Abs) in whole extracts from WT or β2 KO mouse hippocampus (lanes 1 in top two panels). Moreover, affinity purification on α-Bgtx affinity resins isolated comparable levels of α7*-nAChR from WT or β2 KO mouse hippocampus (compare lanes 1 and 3 of Fig. 1A top) but did not isolate nAChR containing β2 subunits (compare lanes 1 and 3 of Fig. 1A, bottom left), which instead were found in the flow-through fraction (lane 2; Fig. 1A bottom left). As expected, no β2*-nAChR were found in extracts isolated on Bgtx resins, or in the flow through from that separation, for tissue taken from β2 KO mice (Fig. 1A lower right panel lanes 1,3 and 2).

Molecular Pharmacology Fast Forward. Published on July 7, 2014 as DOI: 10.1124/mol.114.093377
This article has not been copyedited and formatted. The final version may differ from this version.

In further agreement with the findings of the binding studies, western blot analysis showed that basal forebrain extracts contained fewer α7*-nAChR (i.e., immunoreactive α7 protein) than hippocampal extracts, whereas amounts of immunoreactive β2 subunits was very similar across brain regions. Analysis of the western blots probed using anti-β2 subunit Abs showed clearly-detectable β2 subunit presence in α7*nAChR isolated on Bgtx resins from tissue derived from basal forebrain, but not from the hippocampus (compare lanes 3 of the bottom-left panels of Figs. 1A and 1B). To quantify the % of α7 receptors containing the β2 subunit we loaded on the same gel 10 μg of 2% Triton extract and 1/10 of the α–Bgtx purified receptor and determined by western blotting the optical density of the immunoreactivity of β2 subunit present in the extract (corrected for the total volume used for the receptor purification) and that of the α–Bgtx purified receptor. We found that the immunoreactivity of the β2 subunit determined in the purified α-Bgtx was 2.25 ±0.6 % (n=4) of the total β2 subunit immunoreactivity measured in the basal forebrain extracts of WT mice.

α-Bgtx-binding sites in human brain

The possible presence of α7β2-nAChR in human brain was analysed using post-mortem samples of basal forebrain and cerebellum. In preliminary experiments, we characterised nAChR subtypes expressed in basal forebrain and cerebellum and their levels in 2 % Triton extracts (Table 3). The average level of [^{125}I]-α-Bgtx-labelled (α7*-) nAChR was higher in basal forebrain than cerebellum.

The level of [^{3}H]-epibatidine-binding nAChR in cerebellum depended on smoking status. As shown in Table 3 the density of non-α7*-nAChR measured by means of [^{3}H]-Epi binding was higher in smokers than in non-smokers (p=0.02). Based on immunoprecipitation using subunit-specific Abs, in both tissues the large majority of [^{3}H]-Epi-binding sites contained the β2 subunit associated with the α4 subunit (α4β2-nAChR: 75% in basal forebrain and 60% and 67% in cerebellum of smokers and non-smokers, respectively). An additional 14% of [^{3}H]-Epi-binding sites in the basal forebrain were α2β2*-nAChR whereas

Molecular Pharmacology Fast Forward. Published on July 7, 2014 as DOI: 10.1124/mol.114.093377
This article has not been copyedited and formatted. The final version may differ from this version.

this subtype accounted for only 7% of cerebellar [^{3}H]-Epi-binding sites. The largest region-to-region difference was for α3β2*-nAChR: whereas those sites accounted for 4.8% of [^{3}H]-Epi-binding sites in the basal forebrain, they represented 32% in the cerebellum.

α-Bgtx affinity-purified binding sites were obtained from three human basal forebrain (Fig. 2; lanes 1-3) or three human cerebellum (Fig. 2; lanes 5-7) samples. These sites were western blotted and probed with anti-α7 subunit Abs (top) or two different anti-β2 subunit Abs (anti-β2(1) Abs (middle) and anti-β2(2) (bottom)) targeting different epitopes within the β2 subunit. Control samples were extracts from α4β2-nAChR-expressing, transfected HEK cells (lane 4) or from α7-nAChR-expressing, transfected SH-SY5Y cells (lane 8), also probed with the Abs. Levels of immunoreactivity for the α7 subunit were very similar in samples loaded in lanes 1, 2, 5 and 6, higher in the sample loaded in lane 3, and lower in the sample loaded in lane 7. Similar isolates from HEK-α4β2 cells were negative, but SH-SY5Y-α7 cells contained immunoreactive α7 subunits (Fig. 2 upper panel, lanes 4 and 8, respectively). Isolation of α-Bgtx binding sites also yielded anti-β2 subunit Ab-labeled proteins from basal forebrain samples but not from the cerebellum, regardless of whether the cerebellum samples were obtained from smokers or non-smokers. Such immunoreactivity was absent in extracts from SH-SY5Y-α7 cells but very evident in HEK-α4β2 cells (Fig. 2 middle and lower panels, lanes 8 and 4, respectively). Both the α7 and β2 subunits present in the human tissues show a slightly higher molecular weight then the corresponding transfected subunits. This is probably due to differences in glycosylation between native and transfected receptors.

Since it has been shown in a heterologous expression system that an α7β4-nAChR subtype may be formed (Criado et al., 2012), we also probed human α-Bgtx-purified sites with anti-β4 subunit Abs with proven specificity (Supplementary Figure 2, bottom). No specific labelling was observed in either the human basal forebrain or cerebellum samples, showing absence of α7β4-nAChR. Collectively, these results clearly indicate that α7β2-nAChR are present in the human basal forebrain but not in the cerebellum.

Molecular Pharmacology Fast Forward. Published on July 7, 2014 as DOI: 10.1124/mol.114.093377
This article has not been copyedited and formatted. The final version may differ from this version.

Functional expression of concatemeric α7*-nAChR from human subunits

Heterologous expression has shown assembly of functional α7β2*-nAChR (see Introduction), but the way(s) in which α7 and β2 subunits might combine from individual, unlinked, subunits could not be defined. Accordingly, we used a linked-subunit approach to produce α7*-nAChR with defined subunit ratios and assembly orders. Each of the three concatemeric constructs [$(\alpha7)_5$-nAChR homopentamer, $(\alpha7)_4(\beta2)_1$-nAChR, and $(\alpha7)_3(\beta2)_2$-nAChR] showed concentration dependent ACh-evoked function (representative traces shown in Fig. 3A-D). This function, while smaller than that measured in *Xenopus* oocytes expressing homomeric α7-nAChR from unlinked human α7 subunits (typically > 1 μA at 7 days after mRNA injection) was easily measurable (≈100 – 300 nA peak current response, depending on the construct). The time-course of desensitization / inactivation following a peak response stimulated by 10 mM ACh (maximally-stimulating concentration) was also measured for each construct. For each construct, desensitization / inactivation was best fit by a double exponential decay model. As detailed in the legend to Fig 3 no significant differences were seen between the fast desensitization / inactivation time constants calculated for each group. This is not surprising since the apparent time constants will likely reflect the relatively slow kinetics of agonist application in the apparatus, rather than the much faster kinetics of α7*-nAChR desensitization (Papke, 2010). Indeed the apparent τ_{fast} values are very similar to those measured for solution exchange in our apparatus (Eaton et al, 2014). However, the τ_{slow} value calculated for the $(\alpha7)_3(\beta2)_2$ construct was significantly slower than those associated with the other groups. Thus, despite the admitted disadvantages of measuring kinetic parameters in the *Xenopus* oocyte expression system, there is some evidence that α7β2*-nAChR desensitization may be slower than that of homomeric α7-nAChR.

Agonist and antagonist pharmacology of concatemeric human α7*-nAChR

Pharmacological parameters of selected ligands were determined at concatenated α7*-nAChR. Compounds chosen included the prototypical agonists, ACh and nicotine,

Molecular Pharmacology Fast Forward. Published on July 7, 2014 as DOI: 10.1124/mol.114.093377
This article has not been copyedited and formatted. The final version may differ from this version.

choline (which is a relatively selective agonist of α7 nAChR (Alkondon et al., 1997)), and two further agonists with established selectivity for other β2*-nAChR subtypes (sazetidine-A and CC4 (Kozikowski et al., 2009; Sala et al., 2013; Xiao et al., 2006)). Agonist pharmacological profiles for $(\alpha7)_5$-, $(\alpha7)_4(\beta2)_1$-, and $(\alpha7)_3(\beta2)_2$-nAChR subtypes were largely indistinguishable from each other, and from that for non-concatemeric (loose-subunit), homomeric α7nAChR (Fig. 4; Table 4). The only exception is that nicotine has significantly lower efficacy (normalized to that of ACh) at both α7β2*-nAChR subtypes than at concatemeric $(\alpha7)_5$-nAChR or unlinked α7- nAChR (which are statistically indistinguishable on this measure). There was also a trend towards lower nicotine potency across all concatemeric α7*-nAChR constructs, but this did not reach statistical significance (see Table 4). The observed slight trend towards lower choline efficacy, although not significant, is suggestive of the previous observation of 50-70% efficacy of choline vs. ACh at putative α7β2 nAChR expressed from non-linked subunits (Khiroug et al., 2002; Zwart et al., 2014). Strikingly, both sazetidine-A and CC4 were very weak agonists (< 10% efficacy normalized to that of ACh) at all α7*-nAChR subtypes tested, including both α7β2-nAChR, making it impossible to reliably calculate EC_{50} or Hill slope values from the resulting concentration-response data.

Concentration / response relationships were also explored for archetypal α7 antagonists (MLA and the snake venom α-toxin, α-Cbtx), together with the β2-selective antagonist DHβE and the non-competitive antagonist MECA (Fig. 5). The resulting pharmacological parameters are summarized in Table 5. Similarly to the agonist pharmacology, antagonist responses were statistically-indistinguishable between the α7* subtypes (including between α7-only nAChR expressed from either unlinked subunits, or from the concatenated α7 homopentameric construct).

Molecular Pharmacology Fast Forward. Published on July 7, 2014 as DOI: 10.1124/mol.114.093377
This article has not been copyedited and formatted. The final version may differ from this version.

DISCUSSION

This study provides the first direct evidence that α7β2-nAChR are expressed in the mammalian CNS. This is demonstrated by isolation of Bgtx-binding or α7 subunit-containing complexes also shown to contain β2 subunits from human or mouse forebrain samples. In addition, we have demonstrated for the first time that multiple human α7β2-nAChR isoforms of defined subunit composition have pharmacological profiles similar to each other and to homopentameric α7-nAChR.

Our findings indicate that α7β2-nAChR are found in post-mortem, human basal forebrain but not in the cerebellum. Note that total amounts of α7*-nAChR are < 2-fold different in the two brain regions. Specificity of the anti-α7 or anti-β2 Abs used in western blot analysis of these nAChR is demonstrated by control studies using cell lines transfected with specific nAChR subunits, and by studies using WT and subunit-null mice. We also found α7β2-nAChR expression in mouse basal forebrain but not hippocampus. Our results agree with earlier findings of α7β2-nAChR expression in mouse basal forebrain (Liu et al., 2009), but not with the same investigators' study in mouse hippocampus (Liu et al., 2012). There could be several explanations for these seemingly-discrepant observations. nAChR α7 and β2 subunit mRNAs are co- expressed in both basal forebrain and hippocampal cholinergic neurons (Azam et al., 2003). However, fewer than 3% of β2*-nAChR in WT mouse basal-forebrain extracts (this study) were associated with the α7 subunit. This indicates that the large majority of α-Bgtx-binding sites are homomeric α7-nAChR. Accordingly, we feel that the most-likely explanation for the lack of immunochemically-detectable α7β2-nAChR in mouse hippocampus is that it is even less prevalent than in basal forebrain. The previous electrophysiology experiments (Liu et al., 2012) used brain slices from very young mice, whereas our work used tissue from 4-6 month old mice. Therefore, it is also possible that mouse hippocampal α7β2-nAChR expression levels fall from early life into adulthood. Multiple examples of developmental modulation of nAChR subunit expression (including of α7) have previously been seen (Balestra et al., 2000; Conroy and

Molecular Pharmacology Fast Forward. Published on July 7, 2014 as DOI: 10.1124/mol.114.093377
This article has not been copyedited and formatted. The final version may differ from this version.

Berg, 1998; Flora et al., 2000; Zhang et al., 1998; Zoli et al., 1995).

The use of a linked-subunit approach allowed us, for the first time, to directly assess the effects of defined β2 nAChR subunit incorporation on α7*-nAChR function. Of critical importance, no significant differences in EC/IC_{50} values or efficacy relative to ACh were seen between concatenated or unlinked-subunit homomeric α7-nAChR. This indicates that, as has previously been shown for α3β4*-nAChR (George et al., 2012; Stokes and Papke, 2012), α4β2-nAChR (Carbone et al., 2009; Eaton et al., 2014; Mazzaferro et al., 2011; Zhou et al., 2003), and α6β2*-nAChR (Kuryatov and Lindstrom, 2011) subtypes, introduction of appropriately-sized linkers can be performed without altering nAChR functional pharmacology. Several of these previous studies also showed that concatemeric constructs were assembled correctly. To further confirm correct that concatemers were being assembled correctly and not fragmenting and rearranging into unanticipated functional forms, we also coinjected unlinked β2 subunits containing a gain-of-function mutation (L9'S) in the second transmembrane domain. This additional control has previously been used by us and others (Carbone et al., 2009; Eaton et al., 2014). If concatemer fragments were contributing to the functional nAChR population, the β2-gain-of-function subunit would assemble into resulting α7*-nAChR as previously shown (Khiroug et al., 2002; Murray et al., 2012; Zwart et al., 2014). Therefore, if fragments containing α7 were present, this would result in appearance of a novel α7β2-gain-of-function population with distinctive (more agonist-sensitive) properties. However, no such effect was seen.

It is noted, however, that overall function was reduced when α7-nAChR homopentamers were expressed from a concatemeric construct as opposed to from unlinked subunits. This relative diminution in function of concatenated nAChR constructs has been noted in the previous publications just cited and appears to be a regular feature of using concatemeric nAChR constructs. Importantly, however, both $(\alpha7)_4(\beta2)_1$-and $(\alpha7)_3(\beta2)_2$-nAChR concatemeric constructs expressed more function than did the $(\alpha7)_5$-nAChR concatemer. This is the opposite of the situation where loose β2 nAChR subunits are co-

Molecular Pharmacology Fast Forward. Published on July 7, 2014 as DOI: 10.1124/mol.114.093377
This article has not been copyedited and formatted. The final version may differ from this version.

expressed with α7 subunits (Murray et al., 2012), and replicates an earlier finding in which co-expression of unlinked α5, α3, and β4 nAChR subunits reduced function compared to expression of loose α3 and β4 subunits alone, but incorporation of the α5 subunit into a concatemeric construct actually increased observed function of an α3β4*-nAChR pentameric concatemer (George et al., 2012). As in the previous publication, we suspect that uncontrolled assembly of an unlinked additional subunit (in this case β2) may be deleterious, but directed assembly may result in greater functional expression of the new nAChR subtype. Certainly, the current study provides direct evidence that β2 subunit incorporation into α7*-nAChR is compatible with agonist-induced function.

The pharmacological profiles of α7β2-nAChR were very similar to those of homopentameric α7-nAChR. Even agonists (sazetidine-A, CC4) and an antagonist (DHβE) previously shown to have significant β2*-nAChR selectivity had indistinguishable pharmacology across homomeric α7-nAChR and the two different α7β2-nAChR isoforms. Each of these findings match those very recently published using *Xenopus* oocytes expressing α7 and β2 subunits at a 1:10 ratio (Zwart et al., 2014). The only statistically-significant difference in the present study was a diminution of nicotine's efficacy relative to that of ACh in the two α7β2-nAChR isoforms (also seen by (Zwart et al., 2014)). This nicotine partial agonism further confirms that β2 was incorporated into α7β2-nAChR concatemers as planned and may represent a pharmacological marker for the presence of α7β2-nAChR. The same may be true of the slower desensitization kinetics measured for the $(\alpha7)_3(\beta2)_2$ (Figure 3), although it is important to note the limitations of measuring receptor kinetics in a *Xenopus* oocyte system (Papke, 2010). We note that the similar α7-nAChR vs. α7β2-nAChR potency of DHβE observed by us and (Zwart et al., 2014) does not match the observations made in two previous studies (Liu et al., 2009; Murray et al., 2012). The reason for this discrepancy between the pairs of studies is not clear, but two possible explanations occur. First, the differences previously measured are relatively subtle, so may be hard to reproduce. Related to this point, we note that the Hill-slopes of the α7β2-nAChR DHβE

CRCs (Figure 5A) are shallower than those measured for other competitive antagonists (≤ 1, as opposed to significantly > 1 for MLA and α-Cbtx). This would tend to obscure fine differences in IC_{50} values. Second, other α7 and β2 subunit associations are possible, in addition to those used in the α7β2 nAChR concatemers deployed in this study. It is possible that an α7β2*-nAChR population expressed from unlinked subunits may assemble differently, giving rise to the slightly-different DHβE sensitivity previously measured. This would match the previous experience in which α3β4α5-nAChR pharmacology perfectly matched between concatenated and unlinked-subunit nAChR, but that of loose-subunit α3β4-only nAChR was close, but not identical, between loose-subunit and concatemeric constructs (George et al., 2012). Further work may be needed to understand the (admittedly subtle) pharmacological differences between alternative α7β2-nAChR subunit stoichiometries and association orders.

Overall, however, the functional pharmacology of α7-nAChR and α7β2-nAChR subtypes is remarkably similar. This observation indirectly supports the concept that activation of α7β2-nAChR may be predominantly or exclusively mediated only through agonist binding sites at α7/α7 (not α7/β2) interfaces (Murray et al., 2012). If this is true, it seems unlikely that any competitive agonist could exhibit a significantly-different potency between α7-nAChR and α7β2-nAChR. However, antagonists capable of disrupting the allosteric transitions required for nAChR activation (Celie et al., 2005), and of selectively binding to α7/β2 interfaces, could be valuable in this regard as could be other non-competitive ligands. In the concatemeric $(\alpha7)_4(\beta2)_1$-nAChR construct (subunit order α7-α7-β2-α7-α7), only three α7/α7 subunit interfaces will be retained (between the first two subunits, the last two subunits, and between the first and last subunits which will assemble together to complete the pentameric nAChR structure). In the $(\alpha7)_3(\beta2)_2$-nAChR construct, only the α7/α7 interface formed between the first and last subunits will be retained. At first glance, it may seem remarkable that an α7*-nAChR containing such a diminished complement of putative agonist binding sites could be effectively activated. However,

Molecular Pharmacology Fast Forward. Published on July 7, 2014 as DOI: 10.1124/mol.114.093377
This article has not been copyedited and formatted. The final version may differ from this version.

elegant recent work indicates that nAChR, including α7-nAChR, can be activated effectively by as few as one agonist binding site (Andersen et al., 2013; Rayes et al., 2009; Williams et al., 2011).

That α7β2-nAChR are relatively scarce in basal forebrain does not imply that their role is necessarily insignificant. For example, α6β2*-nAChR expression on SN/VTA dopamine projections comprises < 10% of all β2*-nAChR in dopamine terminal regions (Gotti et al., 2005; Whiteaker et al., 2000), but this subtype is extremely important in controlling local neuronal behaviour and signal processing (Exley et al., 2008; Exley and Cragg, 2008). Cholinergic neurons constitute only a fraction (10-15%) of basal forebrain neurons (Semba 2000) and the proportion of α7β2-nAChR in these neurons may therefore be relatively large. The basal forebrain cholinergic system provides primary cholinergic innervations to limbic and cortical brain structures, and expresses nAChR that participate in the cholinergic transmission and cognitive processes associated with learning and memory (Hernandez et al., 2010; Voytko et al., 1994). One of the most marked pathological changes in AD brain is the degeneration of this cholinergic projection and the consequent reduction in the number of nAChR (Dumas and Newhouse, 2011; Pinto et al., 2011). A number of studies have found that the beta-amyloid (Aβ) peptide (a hallmark of AD) plays a critical role in neuronal degeneration and subsequent memory deficits (Capsoni et al., 2000; Dolga et al., 2009; Fraser et al., 1997; Holtzman et al., 1992; Price et al., 1985; Wenk, 1993). Further, a recent electrophysiological study has demonstrated that Aβ binds with higher affinity to α7β2-nAChR than to α7-nAChR, and that this can produce hippocampal neuronal hyperexcitation (through α7-nAChR upregulation) and subsequent neurodegeneration (Liu et al., 2013).

Post-mortem tissue is an under-used substrate for genetic and/or preclinical studies, and provides a translational element that is difficult to recapitulate in animal models alone (McCullumsmith et al., 2014), This study's definitive evidence that α7β2*-nAChR are found in human, as well as mouse, basal forebrain provides valuable support for the concept that

Molecular Pharmacology Fast Forward. Published on July 7, 2014 as DOI: 10.1124/mol.114.093377
This article has not been copyedited and formatted. The final version may differ from this version.

this subtype may be relevant to the study and etiology of Alzheimer's disease. The similarities in human- and mouse-brain basal forebrain α7β2*-nAChR expression are also supportive of the use of mouse models in this context.

Molecular Pharmacology Fast Forward. Published on July 7, 2014 as DOI: 10.1124/mol.114.093377
This article has not been copyedited and formatted. The final version may differ from this version.

ACKNOWLEDGEMENTS

Cerebellum tissue for this study was provided by the Newcastle Brain Tissue Resource

Basal forebrain tissues were obtained from Dr Emanuele Sher and Dr Rudolf Zwart (Eli Lilly Company). We would like to thank Dr Emanuele Sher and Dr Rudolf Zwart (Eli Lilly Company) for their continuous support and for supply of human basal forebrain samples. We would like also to thank Dr Jenny Court (Newcastle upon Tyne, General Hospital, UK) for supplying human cerebellum tissue.

Molecular Pharmacology Fast Forward. Published on July 7, 2014 as DOI: 10.1124/mol.114.093377
This article has not been copyedited and formatted. The final version may differ from this version.

AUTHORSHIP CONTRIBUTIONS:

Participated in research design: Gotti C.,.Zoli M.,.George A.A.,.Lukas R.J., Whiteaker P.

Conducted experiments: Moretti .M., Pistillo F., and.George AA.

Contributed new reagents or analytic tools: Maskos U., Pistillo F. and Whiteaker P.

Performed data analysis: Whiteaker P. Moretti .M, Pistillo F., George AA. and Whiteaker P.

Wrote or contributed to writing of the manuscript: Gotti C.,.Zoli M., Lukas R.J., Whiteaker P.

Molecular Pharmacology Fast Forward. Published on July 7, 2014 as DOI: 10.1124/mol.114.093377
This article has not been copyedited and formatted. The final version may differ from this version.

REFERENCES

Albuquerque EX, Alkondon M, Pereira EFR, Castro NG, Schrattenholz A, Barbosa CTF, BonfanteCabarcas R, Aracava Y, Eisenberg HM and Maelicke A (1997) Properties of neuronal nicotinic acetylcholine receptors: Pharmacological characterization and modulation of synaptic function. *J Pharmacol Exp Ther* **280**(3):1117-1136.

Albuquerque EX, Pereira EFR, Alkondon M and Rogers SW (2009) Mammalian Nicotinic Acetylcholine Receptors: From Structure to Function. *Physiol Rev* **89**(1):73-120.

Alkondon M, Pereira EFR, Cartes WS, Maelicke A and Albuquerque EX (1997) Choline is a Selective Agonist of α7 Nicotinic Acetylcholine Receptors in the Rat Brain Neurons. *Eur J Neurosci* **9**(12):2734-2742.

Andersen N, Corradi J, Sine SM and Bouzat C (2013) Stoichiometry for activation of neuronal α7 nicotinic receptors. *Proceedings of the National Academy of Sciences* **110**(51):20819-20824.

Azam L, Winzer-Serhan U and Leslie FM (2003) Co-expression of α7 and β2 nicotinic acetylcholine receptor subunit mRNAs within rat brain cholinergic neurons. *Neuroscience* **119**(4):965-977.

Balestra B, Vailati S, Moretti M, Hanke W, Clementi F and Gotti C (2000) Chick optic lobe contains a developmentally regulated alpha 2 alpha 5 beta 2 nicotinic receptor subtype. *Mol Pharmacol* **58**(2):300-311.

Capsoni S, Ugolini G, Comparini A, Ruberti F, Berardi N and Cattaneo A (2000) Alzheimer-like neurodegeneration in aged antinerve growth factor transgenic mice. *Proc Natl Acad Sci U S A* **97**(12):6826-6831.

Carbone AL, Moroni M, Groot-Kormelink PJ and Bermudez I (2009) Pentameric concatenated (alpha 4)(2)(beta 2)(3) and (alpha 4)(3)(beta 2)(2) nicotinic acetylcholine receptors: subunit arrangement determines functional expression. *Br J Pharmacol* **156**(6):970-981.

Celie P HN, K asheverov I E, Mordvintsev D Y, H ogg R C, van N ierop P , van E lk R , van Rossum-Fikkert S E, Z hmak M N, B ertrand D , Tsetlin V , S ixma T K and S mit A B (2005) Crystal structure of nicotinic acety lcholine receptor homolog A ChBP in complex with an alpha-conotoxin PnIA variant. *Nat Struct Mol Biol* **12**(7):582-588.

Conroy W G and Berg D K (1998) Nicotinic receptor subtypes in the developing chic k brain: Appearance of a spec ies containing the alpha 4, beta 2, and alpha 5 gene products. *Mol Pharmacol* **53**(3):392-401.

Criado M, Valor L M, Mulet J, Gerber S, Sala S and Sala F (2012) Expression and functional properties of α7 acety lcholine ni cotinic receptors are modified in the presence of other receptor subunits. *J Neurochem* **123**(4):504-514.

Dajas-Bailador F and W onnacott S (2004) Nicotinic acety lcholine receptors and the regulation of neuronal signalling. *Trends Pharmacol Sci* **25**(6):317-324.

Dolga A M, Granic I, Nijholt I M, Nyakas C, van der Zee E A, Luiten P G and Eisel U L (2009) Pretreatment w ith l ovastatin prevents N -methyl-D-aspartate-induced neurodegeneration in the magnocellular nucleus basalis and behavioral dysfunction. *J Alzheimers Dis* **17**(2):327-336.

Drisdel R C and G reen W N (2000) N euronal α-Bungarotoxin R eceptors A re α7 S ubunit Homomers. *The Journal of Neuroscience* **20**(1):133-139.

Dumas J A and Newhouse P A (2011) The cholinergic hypothesis of cognitive aging revisited again: choliner gic functio nal compensation. *Pharmacol Biochem Behav* **99**(2):254-261.

Eaton J B, Lucero L M, Stratton H , Chang Y, C ooper J F, Lindstrom J M, Luk as R J and Whiteaker P (20 14) The U nique α4(+)/(−)α4 A gonist B inding Site in (α4)3(β2)2 Subtype N icotinic Acetylcholine R eceptors P ermits Differential A gonist Desensitization Pharmacology versus the (α4)2(β2)3 Subtype. *J Pharmacol Exp Ther* **348**(1):46-58.

Exley R , C lements M A, H artung H, McIntosh J M and C ragg S J (2008) a lpha 6-Containing nicotinic a cetylcholine receptors dom inate the nicotine con trol of dopamine

neurotransmission in nucleus accumbens. *Neuropsychopharmacology* **33**(9):2158-2166.

Exley R and Cragg SJ (2008) Presynaptic nicotinic receptors: a dynamic and diverse cholinergic filter of striatal dopamine neurotransmission. *Br J Pharmacol* **153**:S283-S297.

Flora A, Schulz R, Benfante R, Battaglioli E, Terzano S, Clementi F and Fornasari D (2000) Neuronal and extraneuronal expression and regulation of the human alpha 5 nicotinic receptor subunit gene. *J Neurochem* **75**(1):18-27.

Fraser SP, Suh YH and Djamgoz MB (1997) Ionic effects of the Alzheimer's disease beta-amyloid precursor protein and its metabolic fragments. *Trends Neurosci* **20**(2):67-72.

George AA, Lucero LM, Damaj MI, Lukas RJ, Chen X and Whiteaker P (2012) Function of Human α3β4α5 Nicotinic Acetylcholine Receptors Is Reduced by the α5(D398N) Variant. *J Biol Chem* **287**(30):25151-25162.

Girod R, Crabtree G, Ernstrom G, Ramirez-Latorre J, McGehee D, Turner J and Role L (1999) Heteromeric complexes of alpha 5 and/or alpha 7 subunits - Effects of calcium and potential role in nicotine-induced presynaptic facilitation, in *Molecular and Functional Diversity of Ion Channels and Receptors* pp 578-590.

Gotti C and Clementi F (2004) Neuronal nicotinic receptors: from structure to pathology. *Prog Neurobiol* **74**(6):363-396.

Gotti C, Hanke W, Maury K, Moretti M, Ballivet M, Clementi F and Bertrand D (1994) Pharmacology and Biophysical Properties of α7 and α7-α8 α-Bungarotoxin Receptor Subtypes Immunopurified from the Chick Optic Lobe. *Eur J Neurosci* **6**(8):1281-1291.

Gotti C, Moretti M, Bohr I, Ziabreva I, Vailati S, Longhi R, Riganti L, Gaimarri A, McKeith IG, Perry RH, Aarsland D, Larsen JP, Sher E, Beattie R, Clementi F and Court JA (2006) Selective nicotinic acetylcholine receptor subunit deficits identified in Alzheimer's disease, Parkinson's disease and dementia with Lewy bodies by immunoprecipitation. *Neurobiol Dis* **23**(2):481-489.

Gotti C, Moretti M, Clementi F, Riganti L, McIntosh JM, Collins AC, Marks MJ and Whiteaker P (2005) Expression of nigrostriatal alpha 6-containing nicotinic acetylcholine receptors is selectively reduced, but not eliminated, by beta 3 subunit gene deletion. *Mol Pharmacol* **67**(6):2007-2015.

Grady SR, Moretti M, Zoli M, Marks MJ, Zanardi A, Pucci L, Clementi F and Gotti C (2009) Rodent Habenulo-Interpeduncular Pathway Expresses a Large Variety of Uncommon nAChR Subtypes, But Only the {alpha}3{beta}4 and {alpha}3{beta}3{beta}4 Subtypes Mediate Acetylcholine Release, pp 2272-2282.

Griguoli M and Cherubini E (2012) Regulation of hippocampal inhibitory circuits by nicotinic acetylcholine receptors. *J Physiol* **590**(4):655-666.

Halevi S, McKay J, Palfreyman M, Yassin L, Eshel M, Jorgensen E and Treinin M (2002) The C.elegans ric-3 gene is required for maturation of nicotinic acetylcholine receptors. *The EMBO Journal* **21**(5):1012-1020.

Hernandez CM, Kayed R, Zheng H, Sweatt JD and Dineley KT (2010) Loss of alpha7 nicotinic receptors enhances beta-amyloid oligomer accumulation, exacerbating early-stage cognitive decline and septohippocampal pathology in a mouse model of Alzheimer's disease. *J Neurosci* **30**(7):2442-2453.

Holtzman DM, Li YW, DeArmond SJ, McKinley MP, Gage FH, Epstein CJ and Mobley WC (1992) Mouse model of neurodegeneration: atrophy of basal forebrain cholinergic neurons in trisomy 16 transplants. *Proc Natl Acad Sci U S A* **89**(4):1383-1387.

Hurst R, Rollema H and Bertrand D (2013) Nicotinic acetylcholine receptors: From basic science to therapeutics. *Pharmacol Ther* **137**(1):22-54.

Keyser KT, Britto LRG, Schoepfer R, Whiting P, Cooper J, Conroy W, Brozozowskaprechtl A, Karten HJ and Lindstrom J (1993) Three subtypes of alpha-bungarotoxin sensitive nicotinic acetylcholine-receptors are expressed in chick retina. *J Neurosci* **13**(2):442-454.

Khiroug SS, Harkness PC, Lamb PW, Sudweeks SN, Khiroug L, Millar NS and Yakel JL (2002) Rat nicotinic ACh receptor α7 and β2 subunits co-assemble to form functional heteromeric nicotinic receptor channels. *J Physiol* **540**(2):425-434.

Kozikowski AP, Eaton JB, Bajjuri KM, Chellappan SK, Chen YH, Karadi S, He R, Caldarone B, Manzano M, Yuen PW and Lukas RJ (2009) Chemistry and Pharmacology of Nicotinic Ligands Based on 6-[5-(Azetidin-2-ylmethoxy)pyridin-3-yl]hex-5-yn-1-ol (AMOP-H-OH) for Possible Use in Depression. *ChemMedChem* **4**(8):1279-1291.

Kuryatov A and Lindstrom J (2011) Expression of Functional Human alpha6beta2beta3* Acetylcholine Receptors in Xenopus laevis Oocytes Achieved through Subunit Chimeras and Concatamers. *Mol Pharmacol* **79**(1):126-140.

Lendvai B and Vizi ES (2008) Nonsynaptic Chemical Transmission Through Nicotinic Acetylcholine Receptors. *Physiol Rev* **88**(2):333-349.

Lewis A and Picciotto M (2013) High-affinity nicotinic acetylcholine receptor expression and trafficking abnormalities in psychiatric illness. *Psychopharmacology (Berl)* **229**(3):477-485.

Liu Q, Huang Y, Shen JX, Steffensen S and Wu J (2012) Functional alpha 7 beta 2 nicotinic acetylcholine receptors expressed in hippocampal interneurons exhibit high sensitivity to pathological level of amyloid beta peptides. *BMC Neurosci* **13**.

Liu Q, Huang Y, Xue FQ, Simard A, DeChon J, Li G, Zhang JL, Lucero L, Wang M, Sierks M, Hu G, Chang YC, Lukas RJ and Wu J (2009) A Novel Nicotinic Acetylcholine Receptor Subtype in Basal Forebrain Cholinergic Neurons with High Sensitivity to Amyloid Peptides. *J Neurosci* **29**(4):918-929.

Liu Q, Xie XT, Lukas RJ, St John PA and Wu J (2013) A Novel Nicotinic Mechanism Underlies beta-Amyloid-Induced Neuronal Hyperexcitation. *J Neurosci* **33**(17):7253-7263.

Lukas RJ, Changeux JP, Le Novere N, Albuquerque EX, Balfour DJK, Berg DK, Bertrand D, Chiappinelli VA, Clarke PBS, Collins AC, Dani JA, Grady SR, Kellar KJ, Lindstrom JM, Marks MJ, Quik M, Taylor PW and Wonnacott S (1999) International Union of

Pharmacology. XX. Current status of the nomenclature for nicotinic acetylcholine receptors and their subunits. *Pharmacol Rev* **51**(2):397-401.

Mazzaferro S, Benallegue N, Carbone A, Gasparri F, Vijayan R, Biggin PC, Moroni M and Bermudez I (2011) Additional Acetylcholine (ACh) Binding Site at α4/α4 Interface of (α4β2)2α4 Nicotinic Receptor Influences Agonist Sensitivity. *J Biol Chem* **286**(35):31043-31054.

McCullumsmith RE, Hammond JH, Shan D and Meador-Woodruff JH (2014) Postmortem Brain: An Underutilized Substrate for Studying Severe Mental Illness. *Neuropsychopharmacology* **39**(1):65-87.

Murray TA, Bertrand D, Papke RL, George AA, Pantoja R, Srinivasan R, Liu Q, Wu J, Whiteaker P, Lester HA and Lukas RJ (2012) alpha 7 beta 2 Nicotinic Acetylcholine Receptors Assemble, Function, and Are Activated Primarily via Their alpha 7-alpha 7 Interfaces. *Mol Pharmacol* **81**(2):175-188.

Orr-Urtreger A, Göldner FM, Saeki M, Lorenzo I, Goldberg L, De Biasi M, Dani JA, Patrick JW and Beaudet AL (1997) Mice Deficient in the α7 Neuronal Nicotinic Acetylcholine Receptor Lack α-Bungarotoxin Binding Sites and Hippocampal Fast Nicotinic Currents. *The Journal of Neuroscience* **17**(23):9165-9171.

Palma E, Maggi L, Barabino B, Eusebi F and Ballivet M (1999) Nicotinic Acetylcholine Receptors Assembled from the α7 and β3 Subunits. *J Biol Chem* **274**(26):18335-18340.

Picciotto Marina R, Higley Michael J and Mineur Yann S (2012) Acetylcholine as a Neuromodulator: Cholinergic Signaling Shapes Nervous System Function and Behavior. *Neuron* **76**(1):116-129.

Picciotto MR, Zoll M, Lena C, Bessis A, Lallemand Y, Lenovere N, Vincent P, Pich EM, Brulet P and Changeux JP (1995) Abnormal Avoidance-Learning in Mice Lacking Functional High-Affinity Nicotine Receptor in the Brain. *Nature* **374**(6517):65-67.

Pinto T, Lanctot K L and Herrmann N (2011) Revisiting the cholinergic hypothesis of behavioral and psychological symptoms in dementia of the Alzheimer's type. *Ageing Res Rev* **10**(4):404-412.

Price D L, Cork LC, Struble R G, Whitehouse P J, Kitt C A and Walker LC (1985) The functional organization of the basal forebrain cholinergic system in primates and the role of this system in Alzheimer's disease. *Ann N Y Acad Sci* **444**:287-295.

Rayes D, De Rosa MJ, Sine SM and Bouzat C (2009) Number and Locations of Agonist Binding Sites Required to Activate Homomeric Cys-Loop Receptors. *J Neurosci* **29**(18):6022-6032.

Riganti L, Matteoni C, Di Angelantonio S, Nistri A, Gaimarri A, Sparatore F, Canu-Boido C, Clementi F and Gotti C (2005) Long-term exposure to the new nicotinic antagonist 1,2-bisN-cytisinylethane upregulates nicotinic receptor subtypes of SH-SY5Y human neuroblastoma cells. *Br J Pharmacol* **146**(8):1096-1109.

Sala M, Braida D, Pucci L, Manfredi I, Marks MJ, Wageman CR, Grady SR, Loi B, Fucile S, Fasoli F, Zoli M, Tasso B, Sparatore F, Clementi F and Gotti C (2013) CC4, a dimer of cytisine, is a selective partial agonist at α4β2/α6β2 nAChR with improved selectivity for tobacco smoking cessation. *Br J Pharmacol* **168**(4):835-849.

Schneider C A, Rasband WS and Eliceiri K W (2012) NIH Image to ImageJ: 25 years of image analysis. *Nat Meth* **9**(7):671-675.

Stokes C and Papke RL (2012) Use of an α3β4 nicotinic acetylcholine receptor subunit concatamer to characterize ganglionic receptor subtypes with specific subunit composition reveals species-specific pharmacologic properties. *Neuropharmacology **in Press.***(0).

Voytko ML, Olton DS, Richardson RT, Gorman LK, Tobin JR and Price DL (1994) Basal forebrain lesions in monkeys disrupt attention but not learning and memory. *J Neurosci* **14**(1):167-186.

Wenk GL (1993) A primate model of Alzheimer's disease. *Behav Brain Res* **57**(2):117-122.

Whiteaker P, Christensen S, Yoshikami D, Dowell C, Watkins M, Gulyas J, Rivier J, Olivera BM and McIntosh JM (2007) Discovery, synthesis, and structure activity of a highly selective alpha 7 nicotinic acetylcholine receptor antagonist. *Biochemistry (Mosc)* **46**(22):6628-6638.

Whiteaker P, McIntosh JM, Luo SQ, Collins AC and Marks MJ (2000) I-125-alpha-conotoxin MII identifies a novel nicotinic acetylcholine receptor population in mouse brain. *Mol Pharmacol* **57**(5):913-925.

Williams D K, Stokes C, Horenstein N A and Papke R L (2011) The effective opening of nicotinic acetylcholine receptors with single agonist binding sites. *The Journal of General Physiology* **137**(4):369-384.

Xiao YX, Fan H, Musachio JL, Wei ZL, Chellappan SK, Kozikowski AP and Kellar KJ (2006) Sazetidine-a, a novel ligand that desensitizes alpha 4 beta 2 nicotinic acetylcholine receptors without activating them. *Mol Pharmacol* **70**(4):1454-1460.

Yakel J (2013) Cholinergic receptors: functional role of nicotinic ACh receptors in brain circuits and disease. *Pflügers Archiv - European Journal of Physiology* **465**(4):441-450.

Zhang X, Liu CH, Miao H, Gong ZH and Nordberg A (1998) Postnatal changes of nicotinic acetylcholine receptor alpha 2, alpha 3, alpha 4, alpha 7 and beta 2 subunits genes expression in rat brain. *Int J Dev Neurosci* **16**(6):507-518.

Zhou Y, Nelson ME, Kuryatov A, Choi C, Cooper J and Lindstrom J (2003) Human alpha 4 beta 2 acetylcholine receptors formed from linked Subunits. *J Neurosci* **23**(27):9004-9015.

Zoli M, Le Novere N, Hill J and Changeux J (1995) Developmental regulation of nicotinic ACh receptor subunit mRNAs in the rat central and peripheral nervous systems. *The Journal of Neuroscience* **15**(3):1912-1939.

Zwart R, Strotton M, Ching J, Astles P C and Sher E (2014) Unique pharmacology of heteromeric α7β2 nicotinic acetylcholine receptors expressed in Xenopus laevis oocytes. *Eur J Pharmacol* **726**(0):77-86.

FOOTNOTES:

The Newcastle Brain Tissue Resource is funded in part by a grant from the UK Medical Research Council [G0400074], by NIHR Newcastle Biomedical Research Centre and Unit funding awarded to the Newcastle upon Tyne NHS Foundation Trust and Newcastle University, and by a grant from the Alzheimer's Society and Alzheimer's Research Trust as part of the Brains for Dementia Research Project.

This work was supported by the European Union Seventh Framework Programme grant [N° HEALTH-F2-2008-20208] to CG and MZ, from the CNR Research Project on Aging, Regione Lombardia Project NUTEC (NUove TECnologie per il trattamento dell'invecchiamento cerebrale basate sull'utilizzo di nanovettori di cellule mesenchimali adulte e dei loro effetto) [ID 30263049], by a grant from the Italian Ministry of Health [RF2009-1549619] (MZ), and by National Institutes for Health Grant [R21 DA026627] and Barrow Neurological Foundation funding to PW.

[†]M.M., M.Z., and A.A.G. contributed equally to this work.

[§]P.W. and C.G. contributed equally to this work and are joint corresponding authors.

Molecular Pharmacology Fast Forward. Published on July 7, 2014 as DOI: 10.1124/mol.114.093377
This article has not been copyedited and formatted. The final version may differ from this version.

FIGURE LEGENDS:

Figure 1. Western blot analysis of nAChR subunit content in α-Bgtx-purified receptors prepared from 2% Triton X-100 extracts of WT and β2 KO mouse hippocampi (A) and basal forebrain samples (B).

A) α-Bgtx-purified receptors were prepared from mouse hippocampi by incubating extracts with Sepharose 4B covalently bound with α-Bgtx. The bound receptors were recovered from the beads using Laemmli sample buffer. Western blot analysis of 10 µg of 2% Triton X-100 extracts of the hippocampus before (lane 1) and after α-Bgtx purification (lane 2; supernatant), and 1/20 of the corresponding α-Bgtx purified receptors (lane 3; recovered from beads). The blots were probed with an anti-α7 Ab (top) or β2 (1) Ab (bottom)

B) α-Bgtx purified receptors were prepared as described in the legend of Figure 1. Western blot analysis of 10 µg of 2% Triton X-100 extracts of the basal forebrain before (lane 1) and after α-Bgtx purification (lane 2; supernatant), and 1/10 of the corresponding α-Bgtx purified receptors (lane 3; recovered from beads). The blots were probed with an anti-α7 Ab (top) or β2(1) Ab (bottom).

Figure 2. Western blot analysis of α-Bungarotoxin-purified nAChR prepared from human basal forebrain and cerebellum.

α-Bgtx-binding nAChR were purified from the same volume of 2% Triton X-100 extracts of basal forebrain and cerebellum by incubating them with Sepharose 4B covalently bound with α-Bgtx. The bound receptors were eluted using sample buffer, and an identical volume of purified receptors was loaded on the gel. The Western blots were probed with anti-α7 Ab (top) or anti-β2 Ab (bottom).

Figure 3. Representative traces and maximum function (I_{max}) comparison for α7*-nAChR pentameric concatemer constructs

Molecular Pharmacology Fast Forward. Published on July 7, 2014 as DOI: 10.1124/mol.114.093377
This article has not been copyedited and formatted. The final version may differ from this version.

Oocytes were injected with mRNA encoding unlinked α7-nAChR subunit monomers (Panel A) concatenated α7 homopentamers (Panel B), α7β2 nAChR with the β2 subunit in position 3 (Panel C), or α7β2 nAChR with the β2 subunit in positions 2 and 4 (Panel D). Representative two-electrode voltage-clamp recordings are shown in each case, for ACh concentration-response determinations (see Methods for details). Black bars above each trace represent 5 s applications of ACh at a range of concentrations. The time course of receptor desensitization / inactivation during stimulation with a maximally-effective dose of ACh (10 mM) was also investigated for each nAChR construct, using additional groups of oocytes. In each case, the time course was best fit by a double-exponential decay. The fast time constants (τ_{fast}) for desensitization / inactivation were statistically indistinguishable by one-way ANOVA across all four groups (unlinked α7, 436 ± 85 ms; α7-only concatemer, 214 ± 80 ms; α7β2(p3), 312 ± 55 ms; α7β2(p2,4), 247 ± 35 ms; $F[3,11] = 2.06$, $p = 0.16$; $n = 3$ in each group). In contrast, the slow time constant (τ_{slow}) for desensitization / inactivation of the α7β2(p2,4) construct was significantly longer that of the other groups; no other differences were detected by Tukey's *post hoc* comparison ($p < 0.05$). Values were: unlinked α7, 5109 ± 800 ms; α7-only concatemer, 3130 ± 585 ms; α7β2(p3), 5073 ± 638 ms; α7β2(p2,4), 6318 ± 365 ms; $F[3,11] = 5.29$, $p = 0.02$; $n = 3$ in each group.

Panel E, summary of maximal function (I_{max}) measured in each concatemeric nAChR group by stimulation with the full agonist ACh (10 mM). Bars represent mean ± SEM (n = 3). I_{max} values were: α7-only, 83.9 ± 18.6 nA; α7β2(p3), 285 ± 11 nA; α7β2(p2,4), 216 ± 45 nA. Analysis using one-way ANOVA with Tukey's *post hoc* comparison showed that incorporation of β2 subunits resulted in a statistically-significant increase in I_{max} ($F[2,6] = 12.7$, $p = 0.007$; denoted by *). The I_{max} values obtained from the two α7β2-nAChR constructs were statistically indistinguishable from each other.

Figure 4. Agonist concentration response profiles for α7 and α7β2 nAChR.

Oocytes were injected with mRNA encoding unlinked α7 subunits (o), concatenated α7 homopentamers (●) or concatenated α7β2 pentameric concatemers (□ indicates α7β2

nAChR with the β2 subunit in position 3; ■ indicates α7β2 nAChR with the β2 subunit in positions 2 and 4). Oocytes were perfused with nAChR agonists (A) acetylcholine (ACh; $10^{-5.5}$ to 10^{-2}; n =6), (B) choline ($10^{-4.25}$ to 10^{-2}; n= 3), (C) nicotine ($10^{-5.5}$ to 10^{-3}; n= 3), (D) sazetidine-A ($10^{-7.5}$ to 10^{-4}; n=3) or (E) 1,2-bis-N-cytisinylethane (CC4; $10^{-6.5}$ to 10^{-3}; n=3). All responses within each group were normalized to an initial control stimulation with 10 mM ACh. Data points represent mean ± SEM. Drug potency and efficacy parameters were calculated by non-linear least-squares curve fitting to the Hill equation (see Methods). The resulting pharmacological parameters and statistical analyses are summarized in Table 4.

Figure 5. Antagonist concentration response profiles for α7 and α7β2 nAChR.

Oocytes were injected with mRNA encoding unlinked α7 subunits (o), concatenated α7 homopentamers (●) or concatenated α7β2 pentameric concatemers (□ indicates α7β2 nAChR with the β2 subunit in position 3; ■ indicates α7β2 nAChR with the β2 subunit in positions 2 and 4). Before antagonists were applied to each oocyte, a control 10 mM ACh-evoked response was measured. Oocytes were pre-perfused with nAChR antagonists (A) dihydro-β-erythroidine hydrobromide (DHβE; $10^{-6.25}$ to 10^{-3}; n=3), (B) methyllycaconitine ($10^{-10.5}$ to 10^{-7}; n=3), (C) mecamylamine ($10^{-7.25}$ to 10^{-4}; n=3) or (D) α-cobratoxin (α-Cbtx; 10^{-10} to 10^{-7}; n=3). The magnitudes of subsequent 10 mM ACh stimulations were compared to that of the initial control. Data points represent mean ± SEM. Drug potency and efficacy parameters were calculated by non-linear least-squares curve fitting to the Hill equation (see Methods). The resulting pharmacological parameters and statistical analyses are summarized in Table 5.

	Number of cases	Age in Years	Postmortem delay in hours	Male/female
Basal forebrain	4 65.7±	9.4	2 >8 2 (2-6)	3/1
Cerebellum smokers	4 73.0±	3.9	>8	2/2
Cerebellum n on-smokers	4 68.7±	6.6	>8	2/2

TABLE 1: Details of cases sampled for receptor analysis. Values are means ± SEM. There were no significant differences between groups for age.

	[^{3}H]-Epibatidine	[^{125}I]-αBungarotoxin
β2 WT Hippocampus	36.3 ±2.3	37.7 ±2.3
β2 KO Hippocampus	1.0±0.3*	39.9±1.0
β2 WT Basal forebrain	44.5±3.5	15.2±2.5
β2 KO Basal forebrain	0.5±0.2* 15.	1 ±2.6

TABLE 2: Levels of [^{3}H]-Epibatidine and [^{125}I]α-Bungarotoxin binding to 2% Triton X-100 extracts (expressed as fmol/mg of protein) in two different brain areas of WT and β2 KO mice. Values are the Mean ± SEM from three separate experiments. * = Significantly different from $\beta2^{+/+}$ by t-test ($p < 0.001$).

	[^{3}H]-Epibatidine [	^{125}I]-α-Bungarotoxin
Basal forebrain	31.8±8.5 80.7±	7.0
Cerebellum non-smokers	22.5 ±2.6	45.7± 5.1
Cerebellum smokers	39.7 ±5.3*	48.3±6.5

TABLE 3: Levels of [^{3}H]-Epibatidine and [^{125}I] α-Bungarotoxin binding to 2% Triton X 100 extracts (expressed as fmol/mg of protein) in the tw o different hu man b rain re gions. Values are mean ± SEM of the 4 sam ples in each group. * D enotes sign ificant difference s in cerebellar membrane [^{3}H]-epibatidine binding between smokers and non-smokers: unpaired t test: p = 0.02. No significant difference was seen between [^{125}I]-α-Bgtx binding levels in cerebellar samples taken from smokers *vs*. non-smokers, by the same measure.

	Acetylcholine Ch				oline				Nicotine				Sazetidine-A				CC4			
Subtype	n=	log(EC_{50} / M)	n_H E	fficacy	n=	log(EC_{50} / M)	n_H E	fficacy	n=	log(EC_{50} / M)	n_H E	fficacy	n=	log(EC_{50} / M)	n_H	Efficacy	n=	log(EC_{50} / M)	n_H	Efficacy
α7 (unlinked)	6	-3.3 ± 0.2	1.3 ± 0.1	103 ± 3	3	-2.9 ± 0.04	1.9 ± 0.3	87 ± 4	3	-4.6 ± 0.14	2.7 ± 0.5	95 ± 2	3	*nd*	*nd*	3.0 ± 0.5	3	*nd*	*nd*	3.0 ± 1.0
α7-α7-α7-α7-α7	6	-3.5 ± 0.3	1.3 ± 0.1	96 ± 2	3	-2.9 ± 0.17	1.6 ± 0.4	96 ± 8	3	-4.1 ± 0.15	1.7 ± 0.3	84 ± 4	3	*nd*	*nd*	7.0 ± 3.0	3	*nd*	*nd*	6.7 ± 1.6
α7-α7-β2-α7-α7	6	-3.5 ± 0.03	1.3 ± 0.1	97 ± 2	3	-2.9 ± 0.03	1.8 ± 0.2	90 ± 3	3	-4.2 ± 0.15	1.9 ± 0.5	58 ± 3*	3	*nd*	*nd*	3.5 ± 0.5	3	*nd*	*nd*	3.2 ± 0.6
α7-β2-α7-β2-α7	6	-3.3 ± 0.3	1.6 ± 0.3	99 ± 3	3	-2.9 ± 0.12	2.0 ± 0.2	95 ± 2	3	-4.2 ± 0.08	1.9 ± 0.6	55 ± 4*	3	*nd*	*nd*	3.4 ± 0.4	3	*nd*	*nd*	3.5 ± 1.0

TABLE 4: α7*-nAChR agonist pha rmacological p arameters. Agonist logEC_{50}, Hill slope (n_H) and efficacy v alues (relative to a maximally-effective (10 mM) concentration of A Ch) were derived by non-linear least-squares curve fitting of the data shown in Figure 4 to the Hill model. α7-only nAChR expressed in *Xenopus* oocytes from unlinked subunits were used as a cont rol group, to which the functional pro perties of α7-nAChR c oncatemeric cons tructs w ere compared (N-to-C-terminal s ubunit order s ar e show n). V alues are mean ± S EM of the nu mber of indicated replicates (n=). n d = not determinable (reliable curve fi tting is not po ssible for ver y low -efficacy co mpounds). P harmacological parameters m easured for each agon ist were generally i ndistinguishable b etween all four gr oups of oocy tes, w ith on e ex ception: t he re lative efficacy of nicotine w as low er for both α7β2 subt ypes tested compared to the α7 un linked control gro up (although the α7-only concatem er group was not different to the control); One way ANOVA F[3,8] = 34.2, p < 0.001, followed by Dunnett's *post-hoc* test.

	Dihydro-β-Erythroidine			Methyllycaconitine M			ecamylamine			α-Cobratoxin		
Subtype	n=	log(IC_{50} / M)	n_H	n=	log(IC_{50} / M)	n_H	n=	log(IC_{50} / M)	n_H	n=	log(IC_{50} / M)	n_H
α7 (unlinked)	3	-5.2 ± 0.05	-1.0 ± 0.1	3	-8.7 ± 0.1	-1.6 ± 0.2	3	-5.6 ± 0.2		3	-8.6 ± 0.1	2.4 ± 0.5
α7-α7-α7-α7-α7	3	-5.3 ± 0.07	-0.8 ± 0.1	3	-9.0 ± 0.1	-1.6 ± 0.2	3	-6.0 ± 0.2		3	-8.6 ± 0.1	1.3 ± 0.8
α7-α7-β2-α7-α7	3	-5.4 ± 0.10	-0.6 ± 0.1	3	-8.9 ± 0.1	-1.7 ± 0.1	3	-6.0 ± 0.1		3	-8.6 ± 0.1	1.8 ± 0.5
α7-β2-α7-β2-α7	3	-5.4 ± 0.10	-0.7 ± 0.1	3	-8.8 ± 0.1	-1.8 ± 0.1	3	-6.0 ± 0.2		3	-8.5 ± 0.2	1.5 ± 0.6

TABLE 5: α7*-nAChR antagonist pharmacological parameters. Antagonist log IC_{50} and Hill slope (n_H) values were derived by non-linear least-squares curve fitting of the data shown in Figure 5 to the Hill model. Values are mean ± SEM of the number of indicated replicates. Pharmacological parameters obtained for each antagonist were statistically indistinguishable between all four groups of oocytes according to analysis with one way ANOVA.

Figure 1

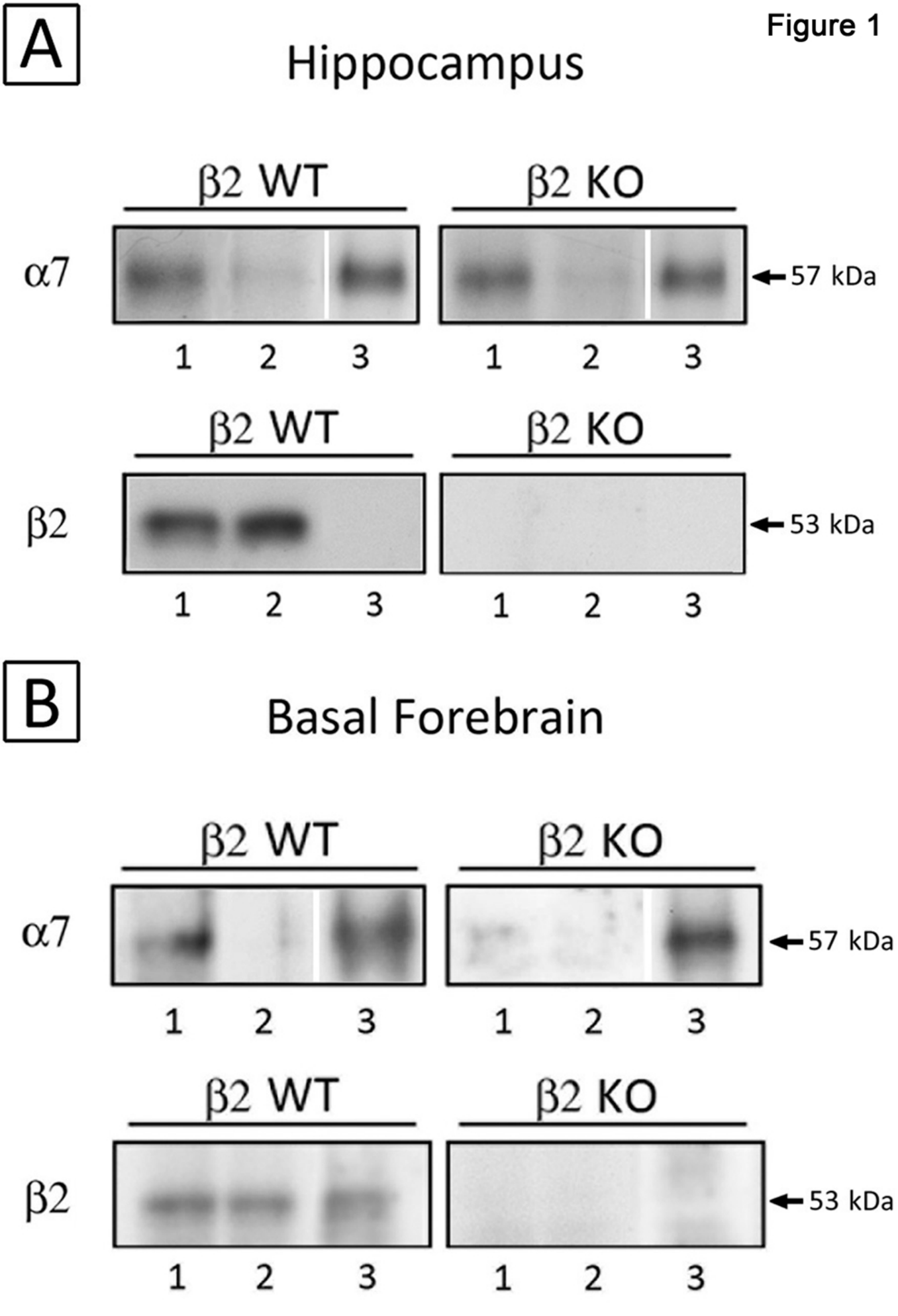
A
Hippocampus
β2 WT
β2 KO
α7
57 kDa
1 2 3
1 2 3
β2 WT
β2 KO
β2
53 kDa
1 2 3
1 2 3
B
Basal Forebrain
β2 WT
β2 KO
α7
57 kDa
1 2 3
1 2 3
β2 WT
β2 KO
β2
53 kDa
1 2 3
1 2 3

Figure 2

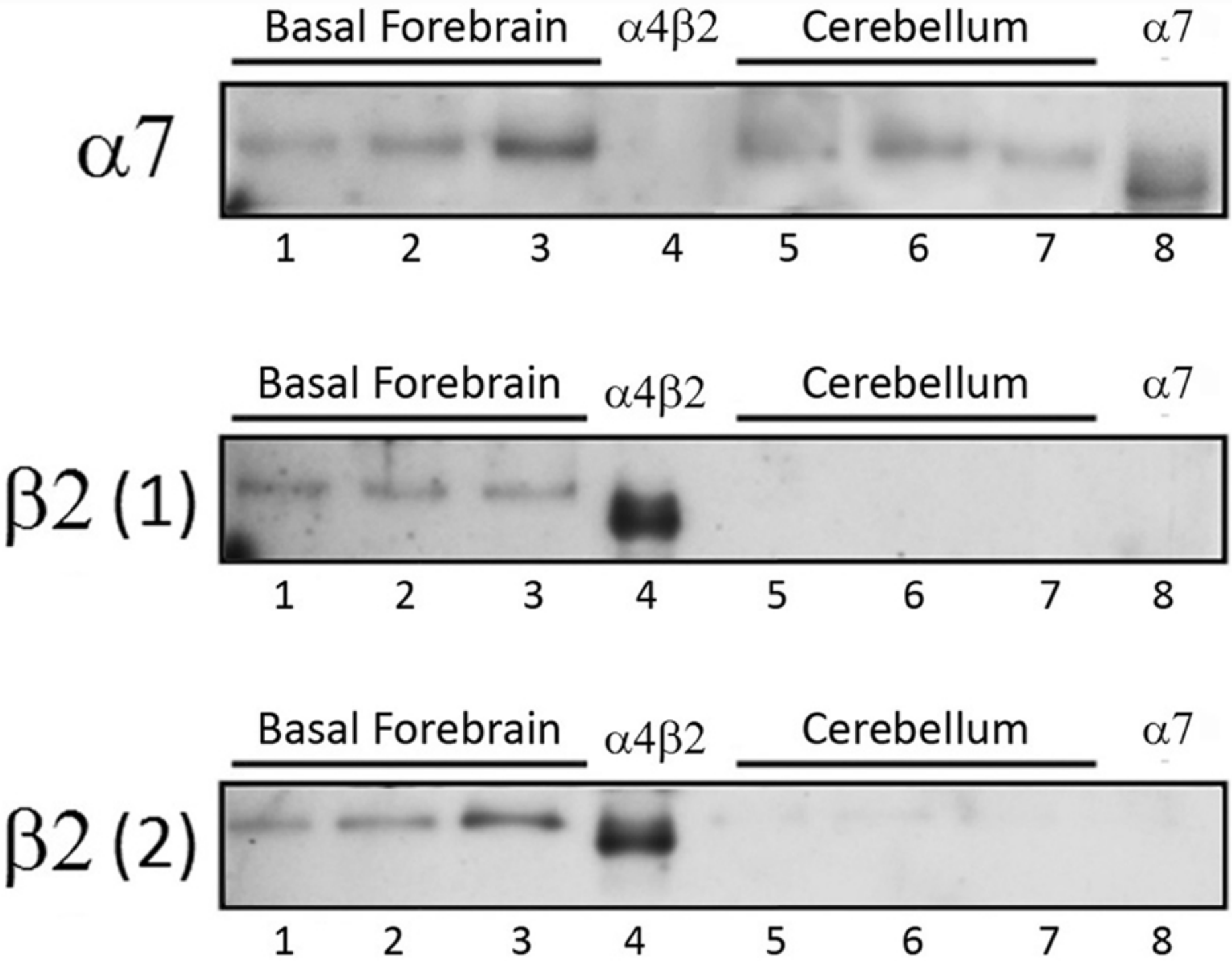
Basal Forebrain
α4β2
Cerebellum
α7
α7
1 2 3 4 5 6 7 8
Basal Forebrain
α4β2
Cerebellum
α7
β2 (1)
1 2 3 4 5 6 7 8
Basal Forebrain
α4β2
Cerebellum
α7
β2 (2)
1 2 3 4 5 6 7 8

Figure 3

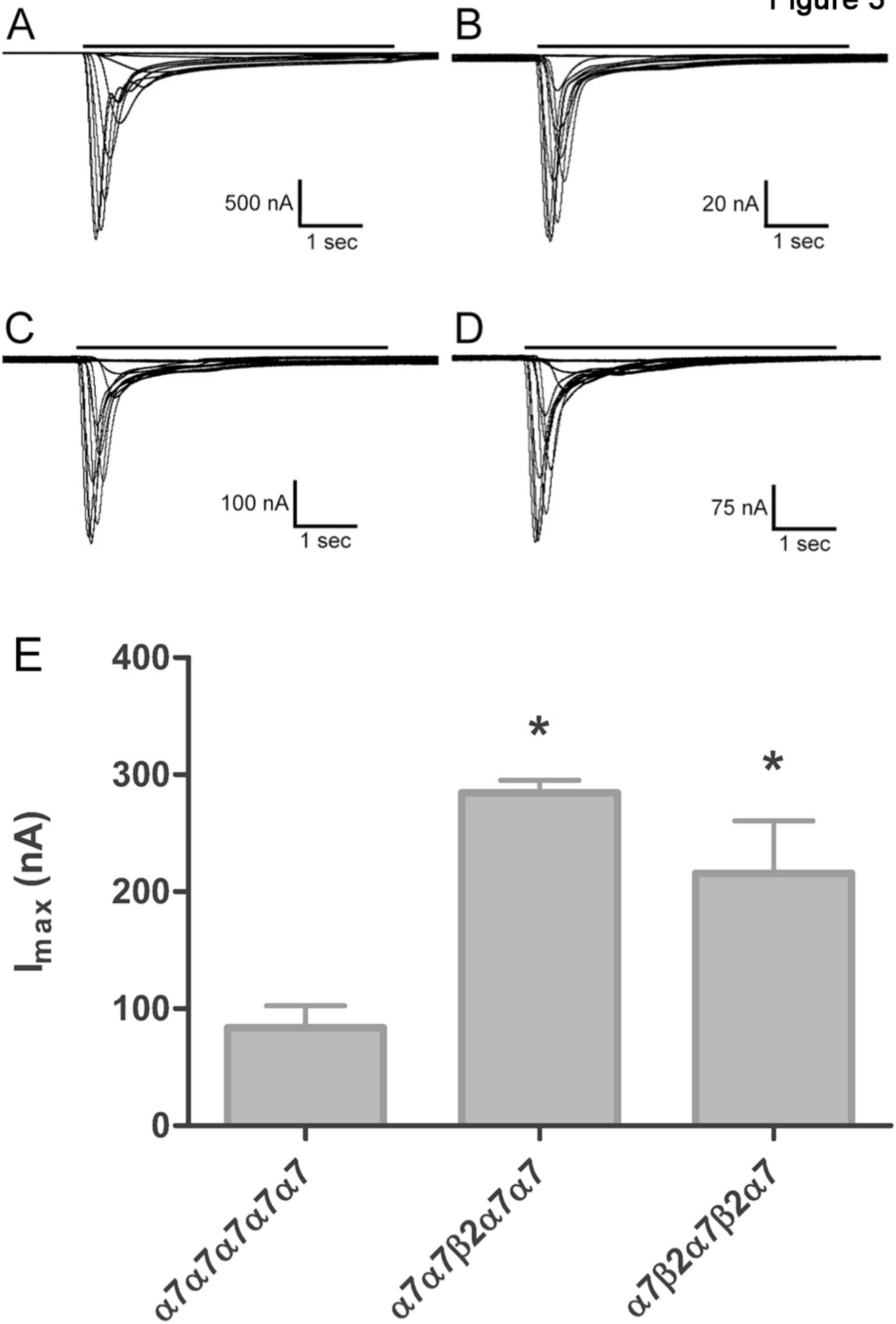
A
500 nA
1 sec
B
20 nA
1 sec
C
100 nA
1 sec
D
75 nA
1 sec
E
400
300
200
100
0
I_{max} (nA)
*
*
α7α7α7α7α7
α7α7β2α7α7
α7β2α7β2α7

Figure 4

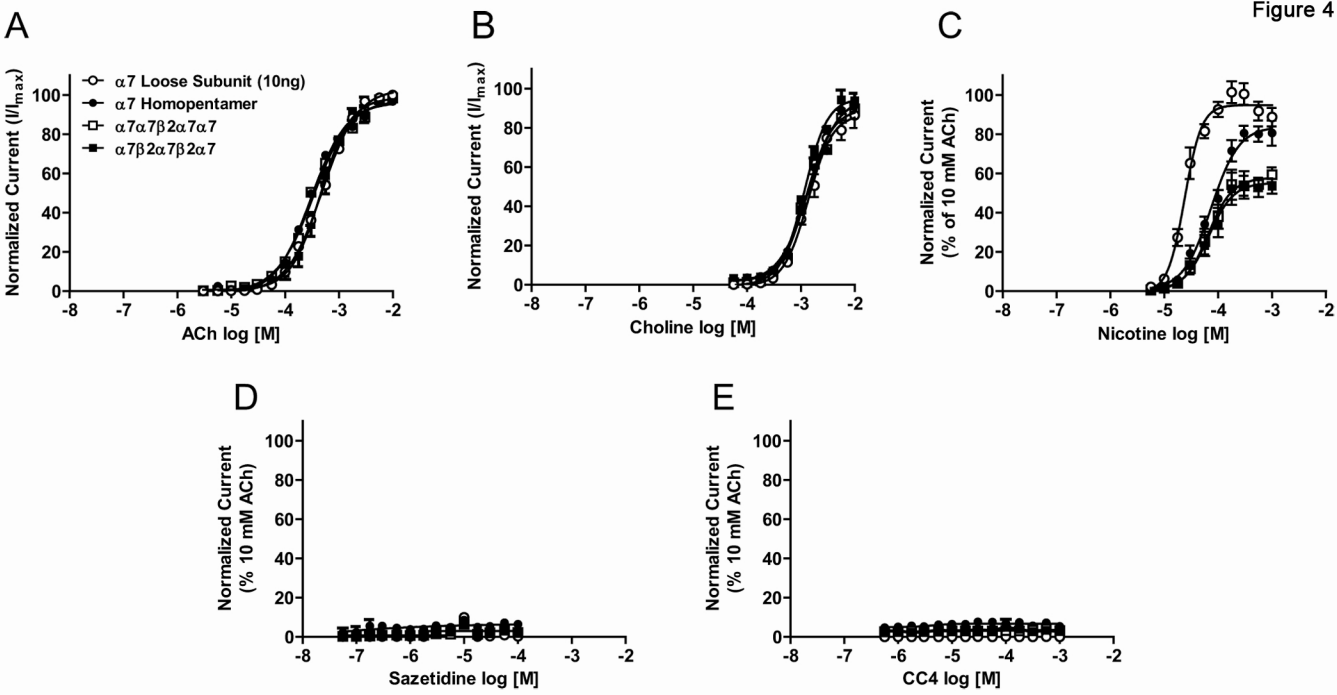
A
α7 Loose Subunit (10ng)
α7 Homopentamer
α7α7β2α7α7
α7β2α7β2α7
Normalized Current (I/I max)
ACh log [M]
B
Normalized Current (I/I max)
Choline log [M]
C
Normalized Current (% of 10 mM ACh)
Nicotine log [M]
D
Normalized Current (% 10 mM ACh)
Sazetidine log [M]
E
Normalized Current (% 10 mM ACh)
CC4 log [M]

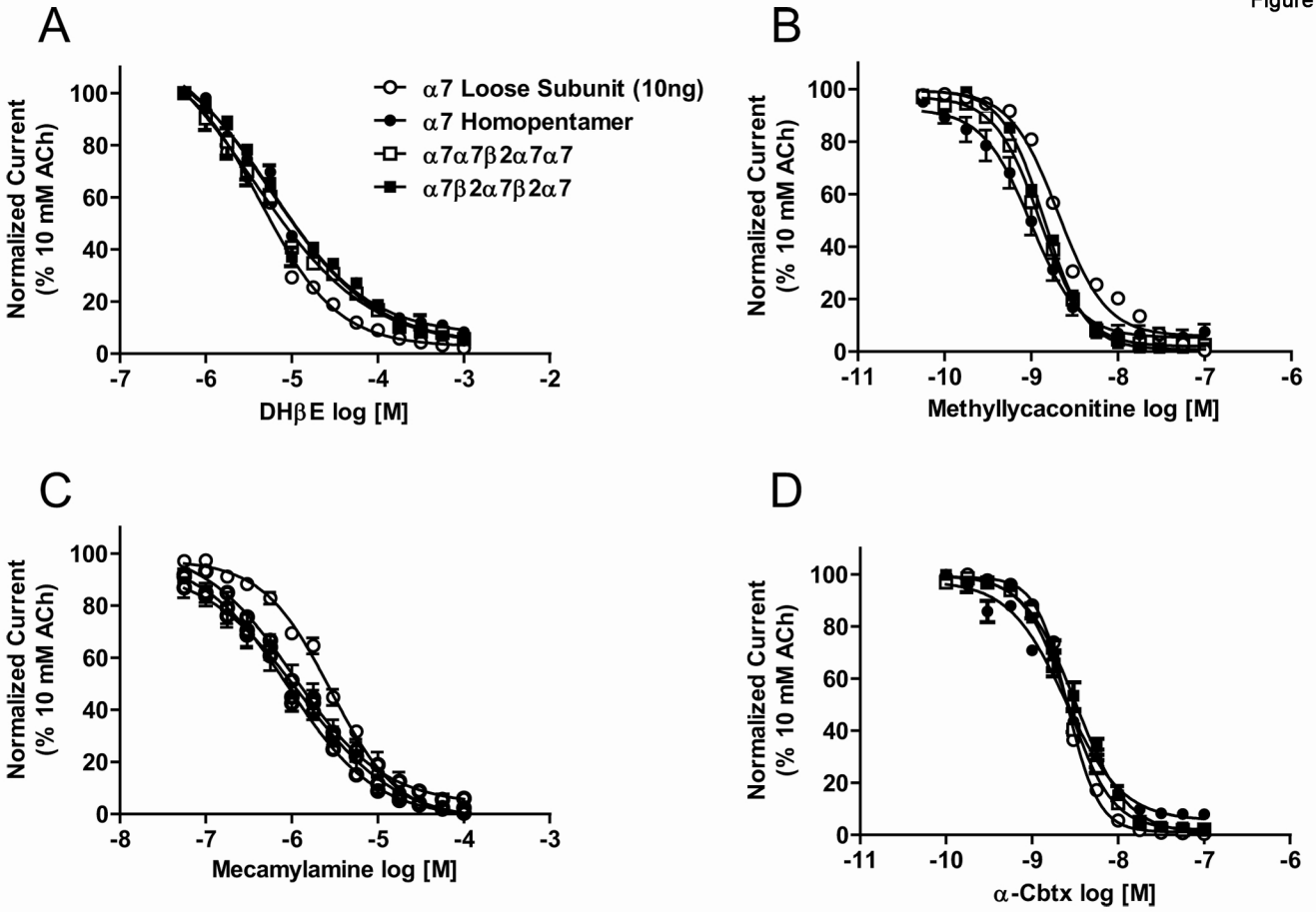
A
Normalized Current (% 10 mM ACh)
α7 Loose Subunit (10ng)
α7 Homopentamer
α7α7β2α7α7
α7β2α7β2α7
DHβE log [M]
B
Normalized Current (% 10 mM ACh)
Methyllycaconitine log [M]
C
Normalized Current (% 10 mM ACh)
Mecamylamine log [M]
D
Normalized Current (% 10 mM ACh)
α-Cbtx log [M]